Mirror Neurons are Modulated by Reward Expectation and Grip Force in the Sensorimotor Cortices (S1, M1, PMd, PMv)

Abbreviated title:

Md Moin Uddin Atique[1] and Joseph Thachil Francis[1-3]

Correspondence: Joey199us@gmail.com

Number of Pages: 53

Number of Figures: 10

Number of Tables:

Number of words for Abstract: 201

Number of words for Introduction: 652

Number of words for Discussion:

Conflict of interest statement: None

Acknowledgements: We thank Matthew J. Perry for helping with the manuscript. Research was supported by NIH 1R01NS092894-01, NSF IIS-17 1527558, DARPA REPAIR Project N66001-10-C-2008.

[1]Department of Biomedical Engineering, Cullen College of Engineering, The University of Houston, Houston, TX 77204, United States;

[2] Department of Electrical and Computer Engineering, Cullen College of Engineering, The University of Houston, Houston, TX 77204, United States;

[3] Lead Contact- jtfracis@uh.edu

Abstract

Mirror Neurons (MN) respond similarly when primates make, or observe, grasping movements. Recent work indicates that reward expectation influences M1 during manual, observational, and Brain Machine Interface (BMI) reaching movements. Previous work showed MN are modulated by subjective value. Here we expand on the above work utilizing two non-human primates (NHPs), one male *Macaca* Radiata (NHP S) and one female *Macaca* Mulatta (NHP P), that were trained to perform a cued reward level isometric grip force task, where the NHPs had to apply visually cued grip force to move and transport a virtual object. We found a population of (S1, M1, PMd, PMv) units that significantly represented grip force during manual and observational trials. We found the neural representation of visually cued force was similar during observational trials and manual trials for the same units, however, the representation was weaker during observational trials. Comparing changes in neural time lags between manual and observational tasks indicated that a subpopulation fit the standard MN definition of observational neural activity lagging the visual information. Neural activity in (S1, M1, PMd, PMv) significantly represented force and reward expectation. In summary, we present results indicating that sensorimotor cortices have MN for visually cued force and value.

Introduction

Mirror neuron (MN)activity has been observed while studying kinematic behaviors, (Gallese et al. 1996; Cisek and Kalaska 2004; Dushanova and Donoghue 2010; G. Vigneswaran et al. 2013), and through indirect measure in human motor cortex (Alaerts et al. 2012). In order to ask questions about force information at the single unit level, we utilized an isometric grip force paradigm with visual grip-force feedback. As MN activity is modulated by variables such as subjective value (Caggiano et al. 2012), and cued reward level (Brandi T. Marsh et al. 2015; An et al. 2019), we

modulated both force and reward level in the current work, while removing any production of kinematics by the subjects.

A better understanding of how reward expectation influences the primary- and pre- sensorimotor cortices has practical implications towards the production of stable and autonomously updating brain machine interfaces (BMIs) (Sanchez et al. 2011; Pohlmeyer et al. 2012; 2014; An et al. 2018; 2019; B. T. Marsh et al. 2015). Neural modulation related to reward has been well characterized within many brain structures (Rolls 2014; Glimcher et al. 2008; Schultz, Dayan, and Montague 1997), and is known to occur at many levels, such as single units and local field potentials (LFP) within M1 (An et al. 2019). The neural response to both reward and conditioned stimuli (CS) that predict reward have been demonstrated in a multitude of brain regions (Zaghloul et al. 2009; Sato and Hikosaka 2002; Cohen et al. 2012; Murray et al. 2008; Tremblay and Schultz 1999; Matthew R. Roesch and Olson 2003; B. T. Marsh et al. 2015; Ramkumar et al. 2016). It has recently been shown that reward expectation changes directional and force related tuning functions within the primary sensorimotor cortices during reaching movements and BCI reaching movements (Zhao et al. 2018; Ramakrishnan et al. 2017). The above studies indicate the need to conduct more research on the influence reward has on these brain regions, and how such variables may modulate MNs. The influence of reward on the primary somatosensory cortex (S1) was reported in preliminary studies (D. McNiel et al. 2016; D. B. McNiel et al. 2016; Atique and Francis 2019). While these experiments demonstrated our ability to classify reward expectation from S1 they did not provide insight on its influence of grip-force during action and action observation. Although a similar reward signal has been demonstrated in primary somatosensory cortex utilizing fMRI, where a stronger BOLD response was recorded for higher reward delivery (Pleger et al. 2008), the investigation of reward-correlated signals within S1 at the single unit level has not been fully developed.

The main goal of the research presented here was to investigate the neural response to reward expectation and reward delivery within S1, M1, PMd and PMv in the presence of a conditioned stimulus (CS, cued) and absence (uncued) of explicit reward-level knowledge to be received for successfully completed trials, during both manual and observational trials. We focused on "grasping" movements with cued isometric grip-force control, to expand beyond reaching movements (Brandi T. Marsh et al. 2015; An et al. 2019). Below we show our ability to decode actual and observed grip-force neural responses during manual and observational trials, as well as reward's influence on the neural population during reward cued and uncued trials. Others have described activity of MNs in M1 during observation of movement (Tkach, Reimer, and Hatsopoulos 2007; Dushanova and Donoghue 2010; Ganesh Vigneswaran et al. 2013; Brandi T. Marsh et al. 2015; Mazurek, Rouse, and Schieber 2018), but not as much has been reported on the activity in S1 during observational tasks, or any of the 4 regions as it pertains to isometric grip-force control while modulating reward level as we do here. Generally, our paper presents findings of MN responses related to varying levels of grip force and reward in M1, S1, PMd and PMv during both manual and observational trials, with stronger responses during manual trials.

Methods

All NHP manipulations described in this work were approved by the Institutional Animal Care and Use Committee of the State University of New York at Downstate Medical Center and conformed to National Institutes of Health (NIH) and United States Department of Agriculture (USDA) animal care and use guidelines. In addition, this work complies with the ARRIVE guidelines. Two non-human primates (NHPs), one 9.0kg male *Macaca* Radiata (NHP S) and one 5.0kg female *Macaca* Mulatta (NHP P), were trained to perform a behavioral grip force task using their right hand/arm and subsequently implanted with 96-channel electrode arrays in S1, M1, PMd and PMv.

Behavioral Task

Both NHPs were trained to perform a grip force task that only required their input during object grasp and transport scenes during manual trials (see Fig.1). Additionally, in manual trials the NHPs had to produce and maintain adequate isometric force while they observed visual grip-force feedback in real-time (Fig.1 red rectangle's width). If NHPs applied the appropriate grip force (indicated by blue rectangular force cues) during object grasp and transport, then released when the object was touching the virtual ground at the target location, the trial was successful. If they did not apply proper force during initial grasp after the go cue, failed to maintain an acceptable force range at any time during the grasp or transport scenes, or released their grip early or late, the trial was considered a failure. The time limit to complete a successful trial was within 10s. The NHPs had to repeat failed trials under the same reward conditions until successful, thus giving incentive to perform non-rewarding trials. Depending on the trial, rewarding (**R1**) or non-rewarding (**R0**), successful execution of the task resulted in delivery of a fluid reward (R1) or lack of reward (R0). Juice rewards were delivered via a system-controlled solenoid driven by task logic (Crist instruments). All elements of the grip force task were developed in Linux using robot operating system (ROS) (Quigley et al. 2009). ROS and Python controlled the task logic, outputs to the reward delivery system, and provided timestamp synchronization with external systems to simultaneously and accurately record task state, reward delivery, and neural data. We analyzed single unit activity from four types of task blocks for each NHP. The four types of task blocks consisted of the following, and in this order for each NHP: first, manually performed tasks with the presence of a reward level conditioned stimulus cue (CS) (manual cued); second, manually performed tasks without a reward level CS (manual uncued); third, observational task with the presence of a reward level CS (observational cued); forth, observational task without a CS (observational uncued).

NHPs were well trained for the grip-force task prior to data collection. NHP S achieved success rates of 89 and 85 percent during the two manual-task blocks, while NHP P achieved rates of 84

and 90 percent. We considered only successfully completed trials for all analyses and results presented in this paper. Successful completion of each R1 trial led to a 0.5s solenoid-controlled fluid delivery. However, successful completion of R0 trials led to no reward, a reset time of 250ms, and progression to the next trial. Some of the recorded blocks contained a visual cue (CS, cued blocks) that indicated whether each trial was rewarding or not, while other blocks were uncued. The start of each trial was marked by the robotic arm traveling to a rest position. During cued blocks, when the robotic arm was at rest, a reward cue “flew” in from the top left side of the screen to indicate a rewarding trial (R1). The visual cue flew across the screen for 0.5s before coming to rest at the top center of the screen, while such a cue was absent during the R0 trials. Also, the absence of a reward during cued blocks further indicated to the NHP that the trial was non-rewarding (R0). All trials (R0 and R1) during uncued blocks lacked a visual reward cue so the NHP had no indication of trial type until the post result period, and thus, no known expectation for reward outcome as the trial sequence was randomized with no clear autocorrelation (see supplementary Fig.S7). For trials that contained a visual reward cue, the post-cue period began immediately after the green visual cue came to rest. In uncued trials, the “post-cue” period began when the robotic arm returned to its rest position from the previous trial.

We defined the post-result period as the time when the cylindrical object was successfully placed at the target location. Feedback was provided to NHPs for successful placement when the blue force squares turned green and the robotic arm released the cylinder during the release scene. Some blocks were performed manually by the NHPs while others required the NHPs to remain attentive and observe the simulated robot arm perform the same type of reach-grasp-transport-release movements performed by the NHPs in the manual trials. NHPs were visually monitored by researchers in real-time via cameras during all sessions to make sure NHPs remained attentive and focused on the projection screen, especially during observational trials. During observational trials NHPs did not have access to the force transducer handle, and their arms were blocked

behind a plexiglass box meant to keep the NHPs hands away from the trainers (BKIN's Arms-Free restraint chair). Additionally, NHPs were trained, and performed all experiments in a dark, quiet, and distraction-free isolation chamber to encourage their attention remained on the large projection screen. Each NHPs' rear-mounted cranial head post was affixed to the BKIN primate chair to restrict head movement for neural recordings. The virtual environment was projected onto a vertical screen in the animal's visual field. Recording sessions were broken into blocks of trials that averaged ten minutes of randomized R1 and R0 trials. The manual blocks consisted of 129 (cued block, 40% R0 trials) and 194 (uncued block, 55% R0 trials) trials for NHP S and for NHP P the numbers were 127 (cued block, 50% R0 trials) and 139 (uncued block, 55% R0 trials). For observational blocks NHP S observed 85 (cued block, 44% R0 trials) and 104 (uncued block, 52% R0 trials), and NHP P observed 50 (uncued block, 56% R0 trials) and 45 (uncued block, 49% R0 trials) trials.

Here, we describe the sequence for one complete trial of the manual reward cued task. We have also provided an illustration of the task phases in Figure 1. After the robot came to the start position, a green square flew in from the left boundary to indicate a R1 trial. Absence of the green square indicated a R0 trial. Next, the robot autonomously moved its arm toward the cylindrical object in the reach scene. At the grasp scene, during manual trials, the NHPs had to apply grip force using a stationary handle that contained a force transducer. The amount of force required was indicated by two blue rectangles (where the inner vertical edge of each blue rectangle indicated minimum force and the outer edges indicated maximum force). As NHPs applied force, visual force feedback was provided via the width of a single red rectangle located directly between the blue force cue rectangles. When the NHPs applied force within the acceptable tolerance range (when the red force rectangle's edges were within the blue rectangles) the robot hand would grasp the object. During transport, the robot arm autonomously moved the object to a predetermined target location, indicated by a pink circle. NHPs had to maintain an acceptable level of grip force during the

transport phase, otherwise the trial was failed and repeated at the same reward level. The mean duration that NHP S applied grip force was 2.5 ± 0.61s (cued), 2.5 ±0.54s (uncued) during manual blocks. During observational blocks the “force” times where 2.1 ±0.26s (cued), 2.2 ±0.27s (uncued). For NHP P, the mean duration was 2.6 ±0.96s (cued), 3.4 ±1.98s (uncued) during manual blocks, and 2.1 ±0.18s (cued), 2.2 ±0.23s (uncued) during observational blocks. After the object was transported to the target location, the NHPs had to release their grip. If all actions were completed successfully the blue rectangles turned green and the NHP was rewarded for R1 trials, but not for R0 trials. Figure 2 depicts a “cued” block trial where reward information was provided to the NHPs.

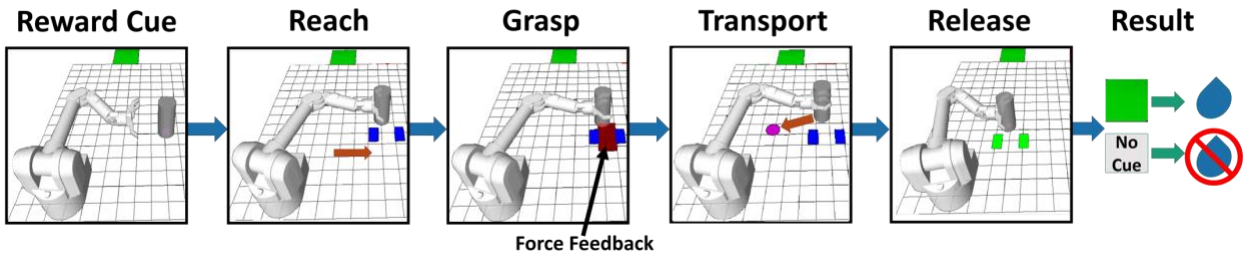

Figure 1: Flow diagram illustrating one reward cued (green square, R1) trial for the grip force task. Absence of the green square indicated a non-rewarding (R0) trial during the cued version of the task. The robotic arm started in the resting position for all trials (left-most image). During uncued blocks, there was no cue provided during the “visual cue” period for any trials. Please note, under experimental conditions with NHPs the background of the grid and free space around the robotic arm and object were black. For the reader’s benefit and visual clarity, both areas have been changed to white here.

Chronic Implantation

We performed implantation procedures as described in-depth in a previous methods paper (Chhatbar et al. 2010), but give a summary here. Following training, when both NHPs achieved

greater than 80% success rate on all trials in a block, the animals were implanted with chronic electrode arrays (Utah array, Blackrock Microsystems) in primary somatosensory (S1, areas 1 and 2), primary motor (M1, rostral) dorsal premotor (PMd) and ventral premotor (PMv) cortices (Fig.2). All surgical procedures were conducted using aseptic technique. NHPs were initially anesthetized with Ketamine, followed by isoflurane and a continuous infusion of fentanyl. The NHP was then placed into a stereotactic frame before the surgical site was shaved and cleaned. An incision was made along the skull to expose desired implant locations. The craniotomy window was large enough to accommodate implant locations while leaving enough margin between the dural flap and skull. The dural flap was kept under tension using stay sutures until electrode arrays were implanted and the site was ready to close. We performed intraoperative probing of S1 to ensure implantation within the hand region, by using a four shank, 32-channel silicon microelectrode array (Kipke et al. 2003) within the post-central gyrus as determined by stereotactic coordinates. The NHP's contralateral hand was continuously stimulated by touch to assess S1 hand region boundaries. Neural responses were amplified and sent to an audio speaker to verify stimulation areas. Utah arrays were then chronically implanted in S1's hand region, in M1 directly reflected across the central sulcus rostral from S1, when possible as large blood vessels can interfere, and in PMd and PMv. The craniotomy was replaced according to previously described methods (Chhatbar et al. 2010).

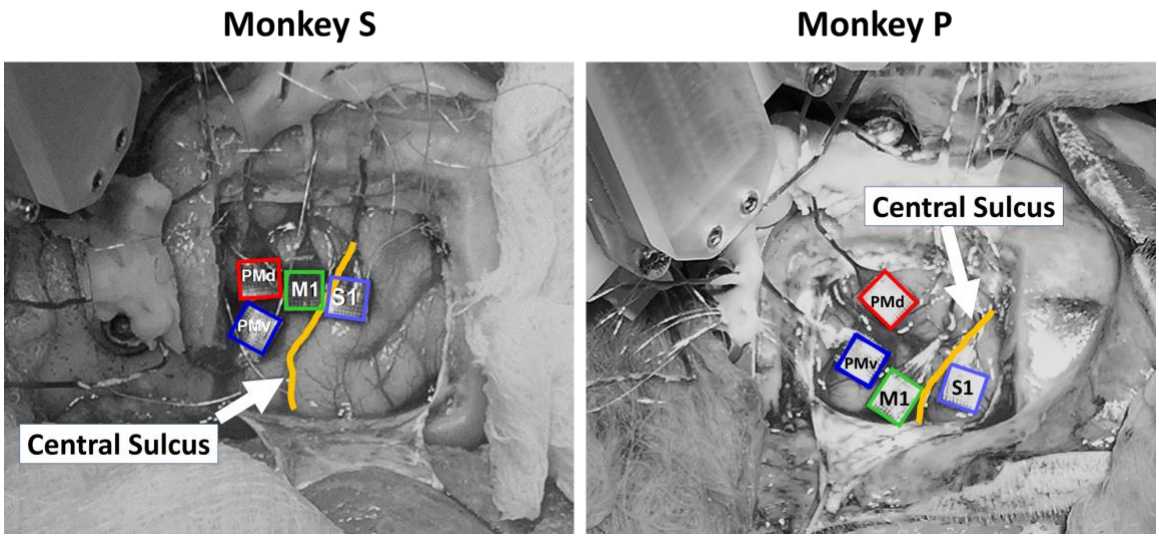

Figure 2: Position of four Utah arrays in relation to the central sulcus for NHP S (left) and P (right). The four arrays were implanted in S1 (light-blue), M1 (green), PMd (red) and PMv (blue) cortices. The green line indicates the Central Sulcus.

Neural Recording

Neural recordings were performed using three synchronized multi-channel acquisition processors (Plexon, Dallas, TX), each having 128-spike waveform recording channels and 32 analogue channels used for simultaneous recording of local field potentials (An et al. 2019; 2018). Single unit recordings were amplified and retained using waveform voltage thresholds. Thresholds were set using an auto-scale (Plexon recording software) feature, followed by manual adjustments that eliminated noise on channels prior to recording. Robot operating system (Quigley et al. 2009) and Python programs controlled task logic and embedded timestamps into neural recordings using a common clock. The common clock was maintained by a microprocessor that delivered a 2kHz pulse to keep task logic and neural data synchronized. Initially, unit waveforms were automatically clustered using a k-means algorithm in principal component space (Kretzberg, Coors, and Furche

2009; Yuan, Yang, and Si 2012). Afterward, we used Plexon's offline sorter software to adjust clusters to remove noise and artifacts.

Significance Related to Reward

We analyzed spike activity in the post-cue and post-result periods separately for cued and uncued blocks to identify units significant for reward modulation. We binned and square root transformed the spike activity into 100ms non-overlapping bins covering 500ms for both the post-cue and post-result periods. We then extracted units that were significant (t-test, $p < 0.05$) for reward expectation (post-cue activity, R1 vs. R0 trials) and reward result (post-result activity, R1 (after reward delivery) vs. R0 (after successful trial with no reward) trials). For reward expectation significance the post-cue activity was 500ms post-cue spike activity when the cue was fully presented (R1 trials) or when the arm reached the resent position from previous trial (R0 trials) and no cue was shown. Finally, we compared spike rate activity between cued and uncued blocks to gain better insight as to how reward feedback information was affected by the presence and absence of a reward cue that is reward expectation based on explicit environmental cues.

Force Trajectory Prediction

We applied linear regression in two steps to identify units that showed significant prediction of grip force from S1, M1, PMd and PMv. In these two steps, the first step identified all units that were significantly related to grip force, which was used below in the sections labeled "*Grip Force Tuning Curve Analysis"* and "*Identifying Observation Modulated Neurons*". The second step was applied to sort out a selective number of the units (from the units collected on the first step) for force prediction to reduce predictor numbers and avoid computational complexity. Unit activity from these cortices were analyzed along with force profiles for both NHPs during manual and observation task blocks (see supplementary material). During some trials, initially the NHP's applied more grip force than necessary and in an effort to meet the target value, reduced their grip force drastically. This resulted in an overcorrection where the NHP had to apply more force to meet

the requirement and resulted in force profiles with multiple peaks. We manually inspected and pruned all force profiles that contained multiple peaks due to highly variable or corrective grip forces applied by NHPs. We defined force onset as the point where force values increased from zero to positive value and force offset when values returned to zero from positive applied force, because the NHPs only grasped the force transducer after the robotic arm reached the virtual object, and a trial was considered successful when they zeroed their output force, let go of the handle, to release the virtual object at the target position. Force data was collected from 0.5s prior to force onset through 0.5s after force offset for all trials. The collected force data was smoothed using a Gaussian kernel (100ms wide). During observational trials the visually cued “force” output profiles were trapezoidal, therefore smoothening gave the force profile a gaussian shape like the force data on manual blocks. From the force data collected in each trial, we evaluated neural spike activity 0.5s prior to, and following each force sample value. This neural activity was further placed into ten non-overlapping time bins centered on each force value (100ms bins, covering 0.5s pre- and 0.5s post-force sample value) to determine a unit’s significance to grip force, so for each unit there were 10-time bins used as predictors. We performed this separately on each unit from all four cortices. We smoothed the raw data using a Gaussian kernel (100ms wide). We wanted a generalized kernel width that would be used for both cued and uncued data blocks of the same kind, manual vs. observational. The force prediction accuracy for different kernel bin widths from 10ms to 250ms was determined for all data. We manually selected the above value of kernel width so that the predictions were close to the peak prediction values for all blocks.

Data recorded from each NHP was split into a fit (90%) and test (10%) set to check goodness of fit and verify predictive performance of the final linear regression model (equation 2). However, before testing the final linear regression model, we extracted significant units related to force in a two-step process. To do this, we subdivided the 90% fit set into 80% (fit) and 10% (validate) data subsets, see the supplementary section for a cartoon of this procedure.

$$\boldsymbol{y_f} = \boldsymbol{a}\mathbf{X}_{fr}^{n_i} + b \quad (eq.1)$$

Equation 1 shows the linear model used, where $\boldsymbol{y}_f$ is the vector of force values, $\boldsymbol{X}_{fr}^{n_i}$ is the binned spike rate for neuron n_i, while $\boldsymbol{a}$ and b are coefficients fit to the data. In the first step, we tested each unit in the 80% subset for the fit related to force using equation 1 and F-test of the model parameters. Units were sorted according to their p-value from the force-fit test and only those with a significant fit ($p < 0.05$) were considered in the second step of the process. For the second step, we took significant force units, starting with the most significant (lowest p-value), and used it to test prediction of force values in the remaining 10% validation subset. We calculated the R-squared value after each unit was added to the model and if the R-squared value increased (improved prediction results), the unit was kept. Remaining units that did not improve the model's force prediction were pruned. After the two-step process, the subset of significant force units was utilized in the final linear regression model (eq. 2). This subset was used with updated coefficients fit to the original 90% dataset. Finally, we used the held out 10% test set to determine prediction and validate accuracy of the linear regression model (eq. 2) by comparing them against actual recorded force values.

$$\boldsymbol{y}_f = \boldsymbol{\alpha}\mathbf{X}_{fr} + \boldsymbol{\beta} \quad (2)$$

The regression model used for final grip force prediction from neural activity is shown in equation 2. Here $\boldsymbol{y}_f$ denotes grip force and $\mathbf{X}_{fr}$ represents binned firing rates for the population of units being used, $\boldsymbol{\alpha}$ and $\boldsymbol{\beta}$ are model coefficients fit to the data.

Grip Force Tuning Curve Analysis

Our previous research concerning force tuning curves in M1 showed a significant difference between R1 and R0 trials (Zhao et al. 2018). We applied the same analysis to our M1, S1, PMd and PMv data to determine if neural activity led to different force tuning curves when taken from R1 vs. R0 trials. As in Zhao et al. 2018 we utilized analysis of covariance (ANCOVA). We analyzed each unit previously identified as significant for force to measure whether the slopes of the tuning curves between R1 and R0 were significantly different (F-test, $p < 0.05$). The p-values from the ANCOVA test are adjusted for multiple comparisons using the false discovery rate (FDR) procedure by Benjamini and Hochberg (BH Method) (Benjamini et al. 1995) for number of hypothesis. The number of hypothesis applied on each unit was 4 and they are, post cue significance (t-test), post feedback significance (t-test), force significance (F-test), and difference between grip force tuning curve (ANCOVA). Significant units identified by ANCOVA were considered to have a force representation that was modulated by reward expectation, and units that also passed the BH method are stated explicitly.

Identifying Observation Modulated Neurons

Our previous work focused on identifying significant units related to reward and/or force within single blocks of data (Zhao et al. 2018) and to expand on these findings, we thought it was important to investigate the cause behind each unit's modulated activity across multiple blocks, during both manual (Zhao et al. 2018), and observational tasks. We hypothesized modulation responses during observation might be explained by the presence of mirror neural activity when NHPs observed the task, received reward, or possibly both. To this end, our goal was to detect units that encoded motor actions (physical application of force), units that responded to cued "force" during visual observation, units that encoded for both and then determine which of these were further modulated by reward level, cued or uncued. We started by identifying and tracking single unit activity across multiple blocks of recorded data. We compared single unit activity

between reward cued manual and observational blocks, and again between uncued manual and observational blocks for each NHP and cortices (S1, M1, PMd and PMv). We tracked single unit activity from the two manual and two observation blocks performed in a single day for each NHP. If a unit on a channel retained the same waveform over all 4 recorded blocks, we considered it the same unit. In addition, we verified this single unit activity by checking the correlation coefficient between the waveform shapes across all blocks, where a high correlation (> 0.98) indicated the same unit. We also confirmed the consistency of single unit activity across blocks by checking the first two principal components using principal component analysis (PCA). Performing these checks allowed us to track single unit activity with significant correlation to reward, force, or both during manual and observation task blocks towards identifying putative mirror neural activity responding to force and reward modulation.

Results

The results section is structured as follows: we start by presenting raw data from manual and observational versions of our task showing peri-event-time-histograms (PETHs) and rasters of sample units, indicating the modulation of single units by both grip-force and reward during manual and observational trials in M1, S1, PMd and PMv, for NHP P and S, Fig.3 and Fig.4 respectively. Next, we present population results from linear regression focusing on grip force, showing that subpopulations of these regions can encode the grip force trajectories (Fig.5) even during observational trials. In Figure 6 we test for temporal shifts between the neural representation of force between the manual and observational versions of the tasks, to determine if the same units are acting in response to the visual input, classical MNs or predicting such input as expected by mental simulation of the predicted visual stimulus, which could be either mental simulation of the expected movement (Cisek and Kalaska 2004), or MNs responding in an anticipatory way due to

the familiarity of the task (Maranesi et al. 2014). Subsequently, we give information on units that are modulated by both force and reward during the force output period of the manual and observational tasks for the same single units that is putative MNs for force and reward.

In Fig.3-4.b1-e1 we present raster plots for example units with all trials aligned to the onset or offset of the grip force. Raster plots aligned to the cue and feedback times are shown in the Supplementary Figures. The mean force profile (indicated with green lines on the raster plots) shows force onset and offset, plotted with arbitrary units for R0 (blue raster) and R1 (red raster) trials. The R0 and R1 mean force profiles are plotted with the same scale for comparison. All four units shown in both Fig.3 and 4, were significant (F-test, $p < 0.05$) for grip force. Plots ax (x=1, 2, 3 and, 4) show the mean spike waveform with standard error (shaded) for a single unit (top) and its PCA space (bottom) for all 4 blocks (Manual and observational, reward -cued and -uncued) recorded on the same day and in the same order for the two NHPs (manual cued (MC), manual uncued (MU), observational uncued (OU) and observational cued (OC)). Each raster subplot (b-e) shows activity for force onset (left) and force offset (right) periods. The dashed horizontal black line on each plot divides the R1 trials from R0 trials. Below the raster plots, solid red and blue lines indicate mean spike rate (Hz) for R1 and R0, respectively. An asterisk (*) indicates a significant (t-test, $p<0.05$, $p<0.01$ and $p<0.001$ denoted by *, ** and *** respectively) difference between either the post force onset or pre-force offset mean spike activity during R1 and R0 trials.

Mirror neuron activity in S1, M1, PMd and PMv (NHP P)

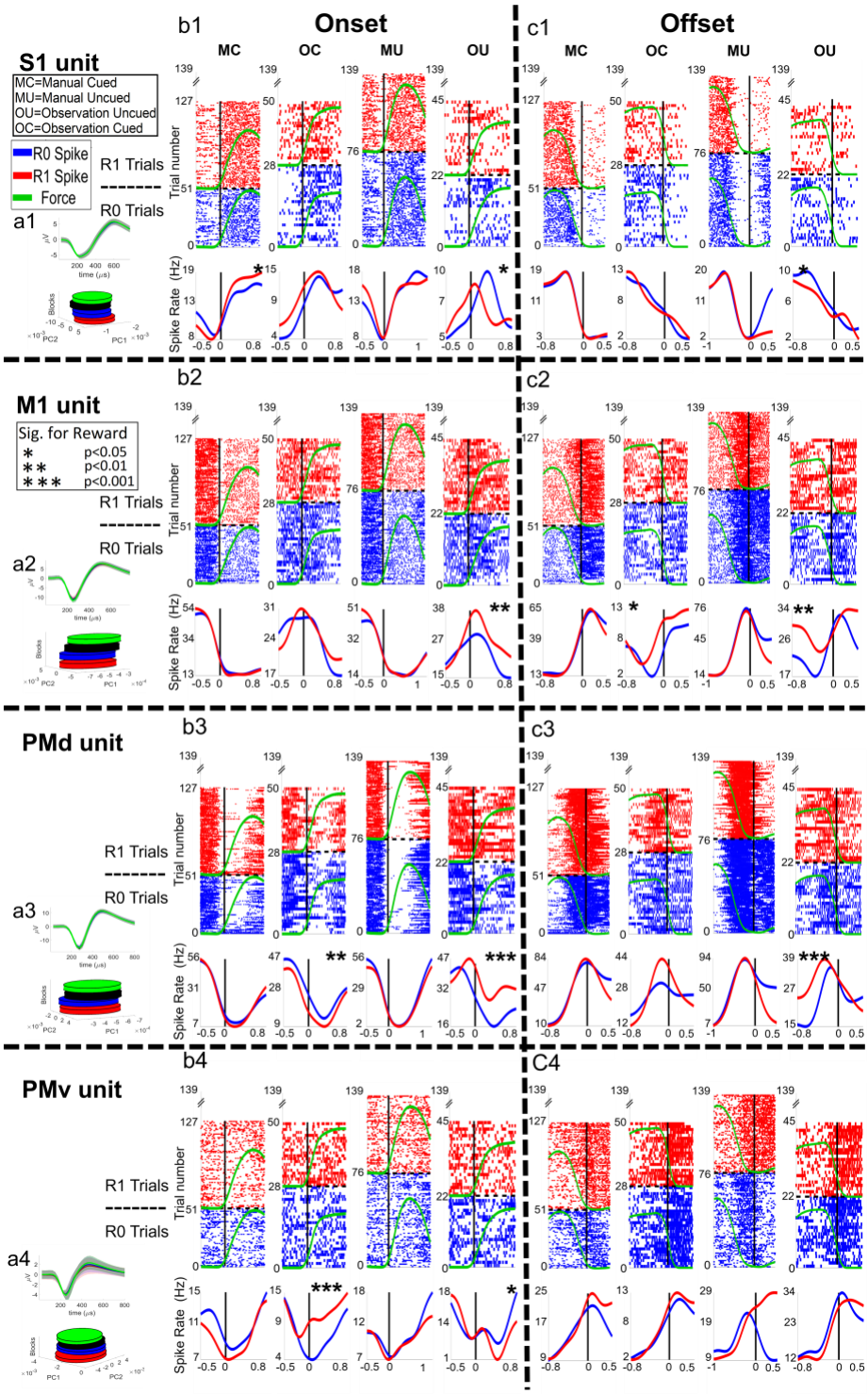

Figure 3: Raster plots of example units from NHP P during the manual and observational blocks. The plot numbers, 1-4, indicate the brain regions (1-4 for S1, M1, PMd and PMv respectively). The letters, a-c, after the numbers, 1-4, are associated with the (a) single unit waveform for an example unit, (b) force onset plots and (c) force offset plots. For (b) and (c) there are four plots for, manual cued task (MC), observational cued task (OC), manual uncued task (MU), and observational uncued task (OU) task sequentially. The post-force onset and pre-force offset time is set as 60% of the mean force length of all trials for that task.

Mirror neuron activity in S1, M1, PMd and PMv (NHP S)

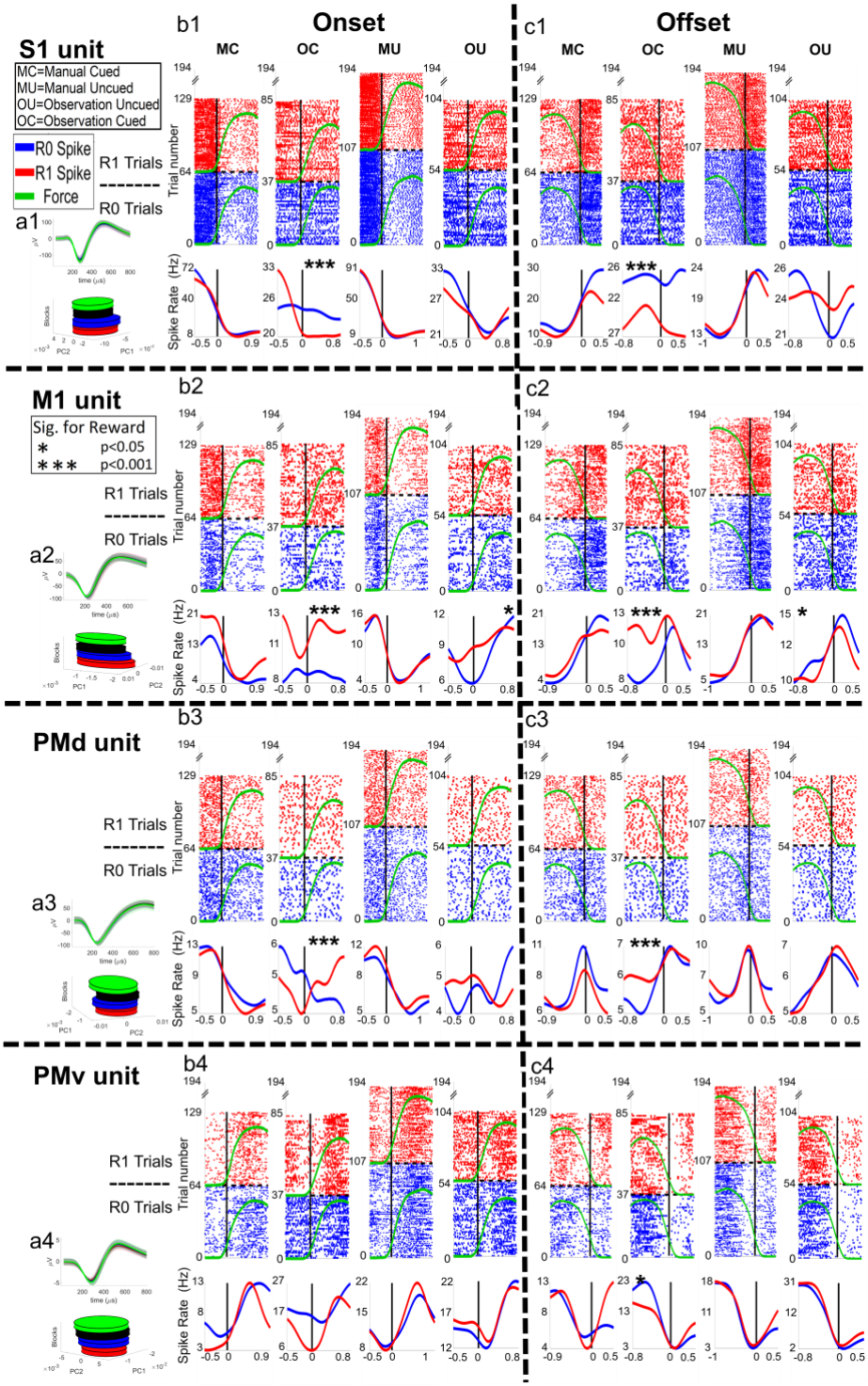

Figure 4: Raster plots of example units from NHP S during the manual and observational blocks. The plot numbers, 1-4, indicate the brain regions (1-4 for S1, M1, PMd and PMv respectively). The letters, a-c, after the numbers, 1-4, are associated with the (a) single unit waveform for an example unit, (b) force onset plots and (c) for force offset plots. For (b) and (c) there are four plots for manual cued task (MC), observational cued task (OC), manual uncued task (MU), and observational uncued task (OU) task sequentially. The post-force onset and pre-force offset time is set as the 60% of the mean force length of all trials for that task.

The observational response to “force” was weaker compared to the actual force experienced during manual trials and did not always align with the force onset and offset times as precisely. All units seen in Figs.3-4 had significant fits to grip force (F-test, $p < 0.05$). This F-test was performed on the regression model (equation 1) to test whether it was a better fit than a degenerate model, which consisted of only a constant term. Figs. 3-4 show a total of 8 example units; 1 from each cortical region (M1, S1, PMd and PMv) for each NHP, P and S, from reward cued, and uncued blocks.

Grip Force Decoding During Manual and Observational Trials

As described in the methods section and further in the supplementary section, data blocks were analyzed using a two-step process. We identified significant units related to force using F-statistics ($p < 0.05$) using the model described in equation 1. Note, we utilized neural data from -0.5s to 0.5s in 100ms bins for this regression. We extracted single units with activity that improved the decoding of force. Linear regression model variables α_i (10 per unit) and β_j were updated using least-squares estimates from 90% of the recorded data. The remaining 10% was used as a test set to verify the performance of force decoding. The R-squared values for the decoding on the test set of force are

shown below. We found high prediction accuracies for both NHPs. The results shown in Fig.5 are force decoding prediction from S1, M1, PMd and PMv cortices for cued manual blocks, top two rows, with the corresponding observational versions seen in the bottom two rows. It is clear the manual tasks generally had higher levels of prediction as compared to the observational versions. Below in Fig. 6 we show the total percentage of units from each region that were significant for predicting force under both the manual and observational versions of the task.

Neural Decoding of Force (Manual and Observational)

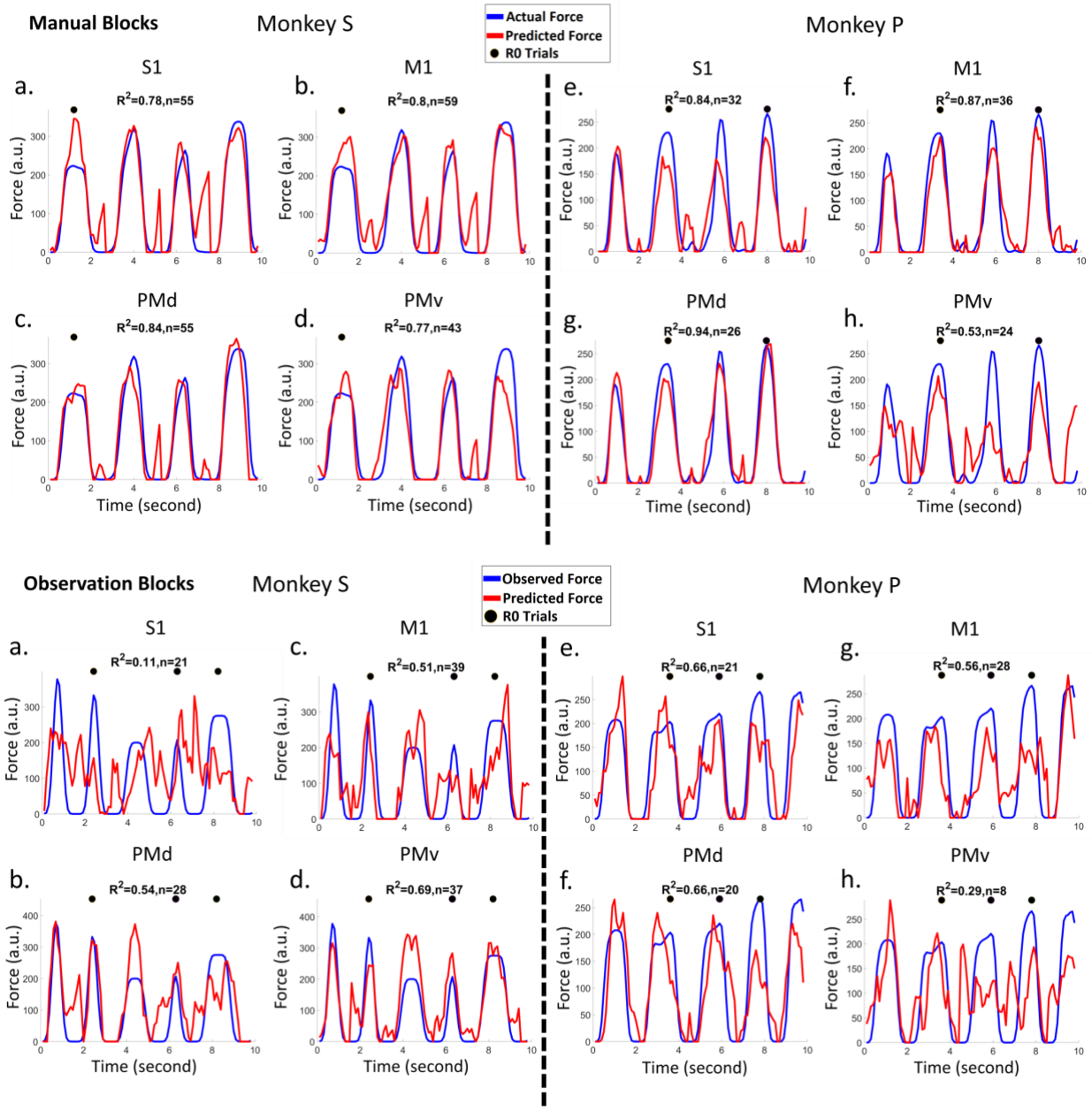

Figure 5: Force decoding (Red lines) from subpopulations of S1, M1, PMd, and PMv cortical recordings taken from manually performed blocks (Blue lines) top two rows, and observational blocks bottom two rows. Linear regression (eq. 2) was used to predict the force. The black dots on each plot indicate that force profile was taken from an R0 trial, while all others were R1 trials. Plots *a, b, c* and d show results for NHP S, for S1, M1, PMd and PMv cortices respectively. Plots e*, f, g,* and h show similar results for NHP P. The top of each figure shows R-squared values (R^2) using

the 10% test set and the number (n) of significant units used for regression to predict force. See table S2 for full stats on the regression models.

% Units with Mirror Neuron Properties Significantly Decoding Force

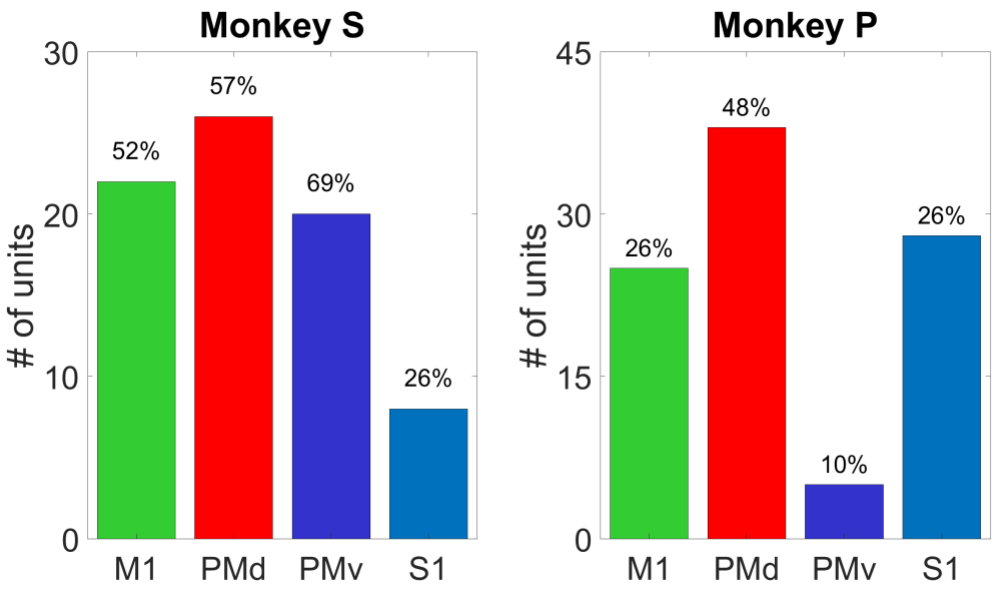

Figure 6: Number of well isolated single units from S1, M1, PMd and PMv that were significant (F-test, BH adjusted for number of hypothesis = 4) for decoding the force time series during both the manual and observational pairs of data sets, which included the pair of manual and observational cued, and the pair of manual and observational uncued versions of the tasks, for the same single units, compared within a task pair, for each NHP. Note this differs from the results in Fig.5 and table S2, which are from regression models using a population of units. The y-axis shows the number of units and on top of each bar the percentage of all well isolated single units for that brain region is given.

Distribution of Peak Significant Correlation Time Lags Between Neural Activity and Force

The analysis in this section was conducted in order to determine if there was an obvious shift in time lag between the neural correlates of force between manual trials and observational trials. One

would expect the neural data responsible for force production, or imagining force production, to lead the force output, whereas classical MN activity would lag the viewed “force” output. However, this may not be the case for predictable movements, such as used in our task, as described by others (Maranesi et al. 2014), where MNs can still lead the observed task. In Fig.7 we have plotted the shift in time lags for the peak time bin significantly correlated with the force trajectories. We asked if these distributions significantly (signed Rank test, $p < 0.05$) deviated from zero between the manual and the observational versions of both the cued and uncued tasks. There were no significant shifts in the histograms for NHP P. NHP S showed three tasks with significant shifts for S1, PMd and PMv. For each plot the zero-time shift shows the probability of a unit not shifting in time between manual and observational. The positive differences are the classical MN response where observational neural activity lags the visual information, whereas, the negative time shifts represent the probability of the observational neural response being earlier, or more “predictive” of moment, than during the manual trials. For more on correlational analysis see Fig.S3 and Fig.S4.

Changes in Neural Time Lag (Observational vs. Manual)

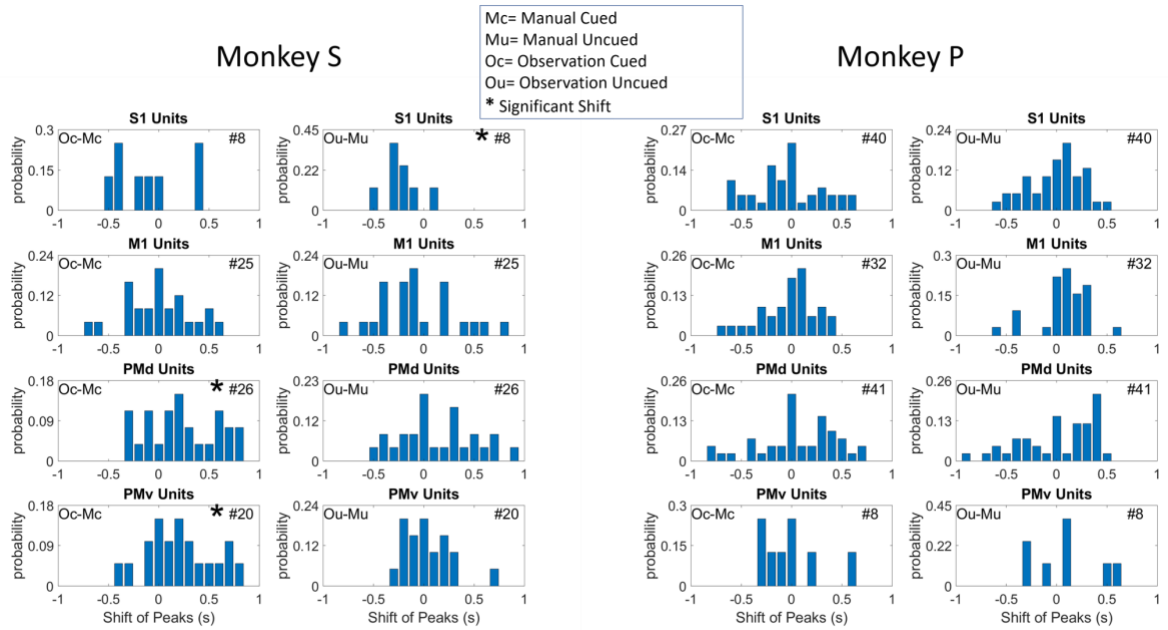

Figure 7: Changes in neural time lags where neural data best correlate with peak grip force. Bar plots showing the shift of peak correlation between similar (cued/Uncued) Manual and Observational blocks for S1, M1, PMd and PMv cortices (cortex is labelled on the title of each subplot). The shift from a block type to another block type (manual-to-observational) is at the top right of each subplot for each NHP (Mc= Manual Cued, Mu= Manual Uncued, Oc= Observation Cued, Ou= Observation Uncued). The number of units used is indicated in the upper right corner of each subplot. The left column for each NHP shows the shift between cued blocks and the right column shows the shift between uncued block. An Asterix (*) symbol before the number of units represents a significant shift in histogram from manual to observational tasks. Probability of unit shifts was calculated by subtracting the position of the peak correlation time bin for observational from the manual tasks for the same unit. For more on this correlational analysis see Fig.S3 and Fig.S4.

Force, Reward and Comodulation of Single Mirror Neurons

Figure 8 shows the number and percentage of units that were significantly correlated with force or reward separately, as well as units that were significant for both simultaneously, and these same units were significant under both manual and observational trials. Single unit activities were tracked across manual and observational cued and uncued blocks to determine the significance of their correlation with force under these different conditions. To clarify, a unit that was present during both cued manual and cued observational blocks was checked for significant correlation with reward and force and included in Fig.8 only if it was significant for both manual and observational trials towards possible discovery of mirror units. The same procedure was performed for uncued manual and observational blocks separately. The plots in Fig.8 show the total number of units (left y-axis) and percentage (top of each bar) for each category that was identified from S1, M1, PMd and PMv recordings. The red bars are for cued trials while the blue bars are for uncued trials. The

analysis windows in Fig.8 for reward were, from post-cue for 0.5s, and post-result for 0.5s while for force significance the window was 0.5s starting at pre-force-onset and for 0.5s after post-force-offset. Note these time windows where not overlapping, thus Fig. 8 is not describing results of force tuning modulation by reward, which is described in Fig.9.

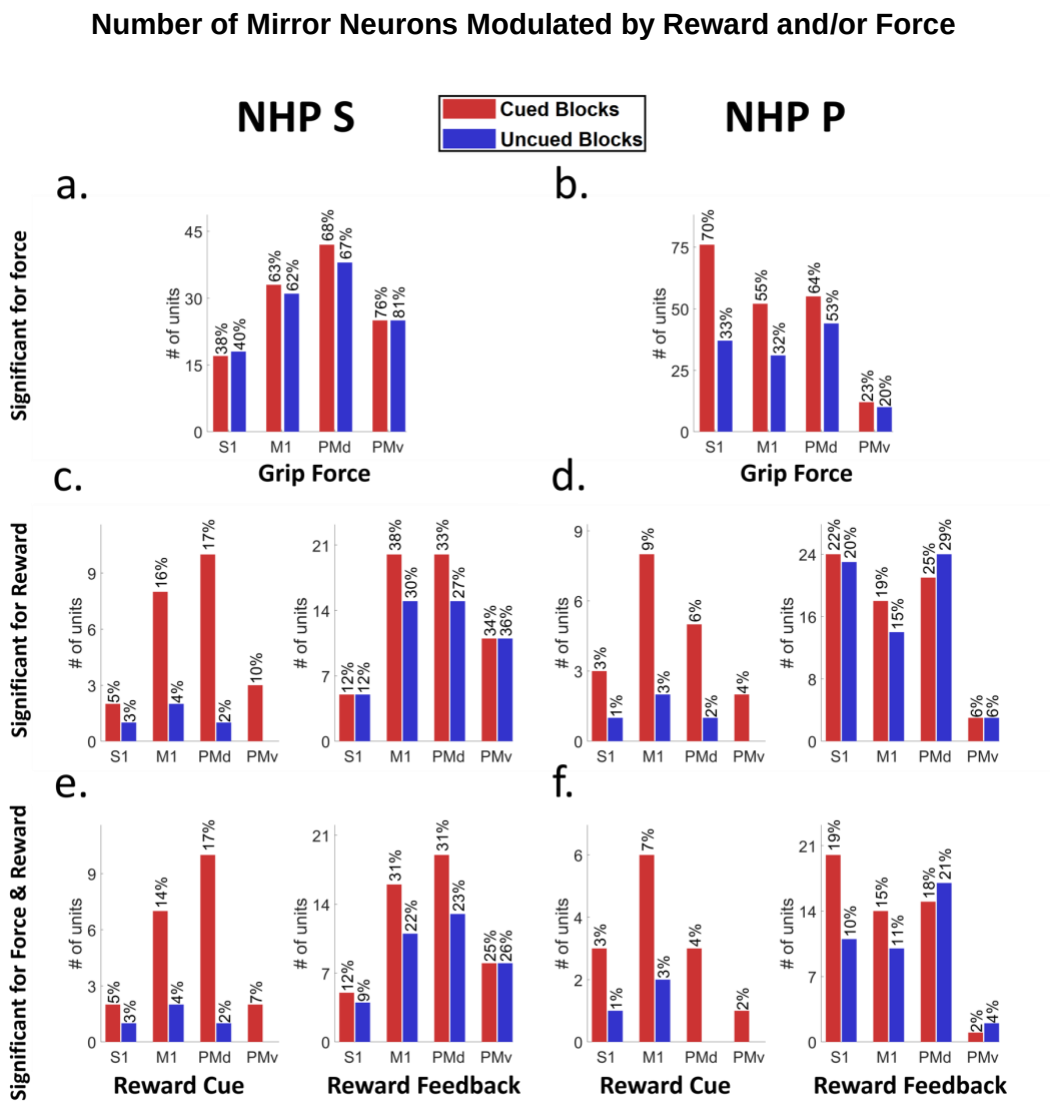

Figure 8. Mirror Neurons in S1, M1, PMd and PMv Encode Reward and Grip Force. The number of units with significant modulation via either grip force (F test, BH method), reward (post-cue or post-reward, t-test, BH method), or both, during manual and observational blocks of a similar type

(e.g. cued or uncued). Red represents units for cued blocks and blue for uncued blocks. Each subplot shows the number of significant units between cued/uncued manual and observational blocks for Force (plot a and b), Reward (plot c and d) and significant for both force and reward (plot e and f). For subplots c, d, e and f the left plot shows units for post reward cue and right plot shows unit for post reward feedback activity. The number of hypothesis tests for BH method was equal to 4, which were the four tests applied on each unit (post cue significance, post feedback significance, grip force significance, and significant tuning curve difference). The BH method is described in the method section titled “grip force tuning curve analysis”.

Modulation of Force Tuning Curves by Cued Reward Level

Force tuning curves for rewarding and non-rewarding trials and significant differences between their slopes were calculated as described in the methods using MATLAB’s ANCOVA function. F-statistics were conducted on the reward group*force interaction which expresses the difference in slopes and the p-value for that interaction was collected. Figure 9 shows the force tuning curves for example units recorded from cued observational blocks for each brain region (see Fig.S5 for the manual version). It shows the relationship between R1 and R0 trials as spike rate varied with force. Note this is in comparison to the previous sections when force decoding meant the neural activity could be used to determine the force level, whereas here we are looking at the change in firing rate as a change in force level and its modulation by reward (encoding). Subplots (Fig.9) to the left side of each sub-figure show smoothed spike rate against force, while the line graphs to the right show force tuning curves obtained from R0 and R1 data. The two example units from each NHP, S and P, had a significant difference between R0 and R1, in agreement with our previous M1 results (Zhao et al. 2018).

Spike Rate vs Force (Observational)

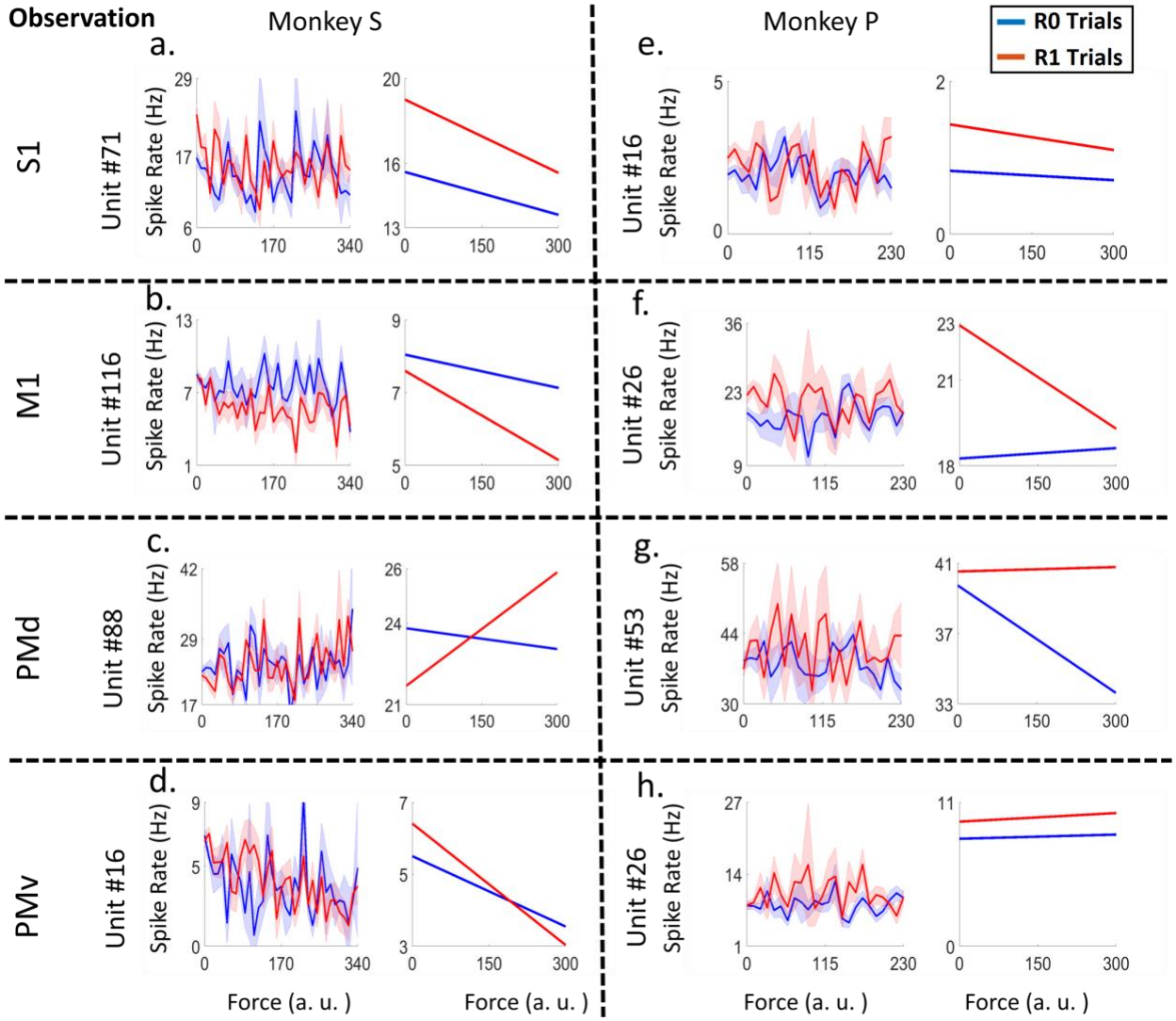

Figure 9: Plots of spike rate vs force (left subplots) and their linear tuning curves (right subplots) for example units from S1 (plot *a, e*), M1 (plot *b, f*), PMd (plot *c, g*) and PMv (plot *d, h*) cortices of both NHPs (for NHP S plots *a, b, c* and *d* and for NHP P plots *e, f, g* and *h*). The units presented here had significant differences between R0 and R1 groups (ANCOVA, F-test, $p<0.05$) force tuning curves during manually performed blocks. Red lines indicate rewarding trials (R1) and blue indicate non-rewarding trials (R0). See Fig.10 for population results and Fig.S5 for the manual version of this figure.

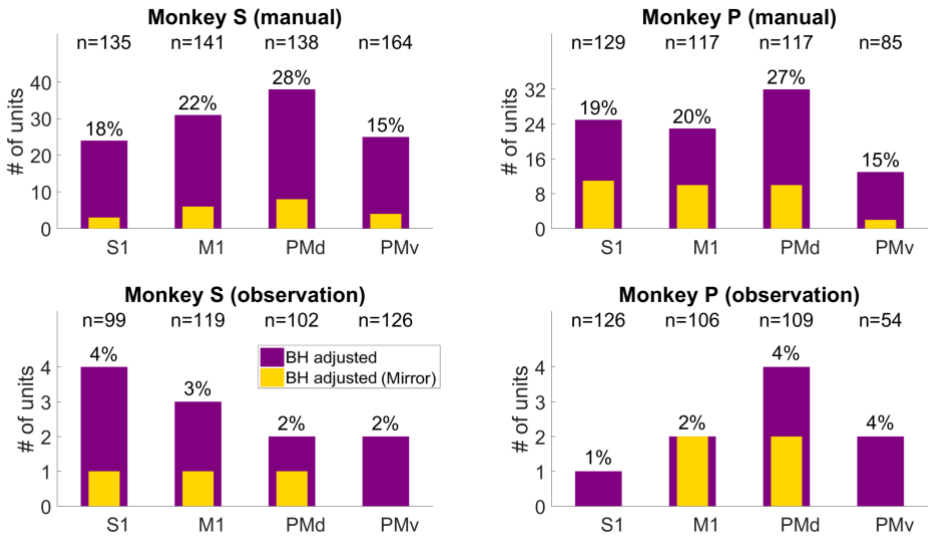

Figure 10: Units with significantly different force tuning curves between R0 and R1 trials. The titles represent which NHP and block type was plotted, p-values were adjusted using the Benjamini-Hochberg method (BH method) correcting for false discovery rate where the correction was applied using p=0.05. The number of hypothesis tests for BH method was equal to the 4 test applied on each unit (post cue significance, post feedback significance, grip force significance, and significant tuning curve difference). The yellow bar inside the purple bar is showing the number of MNs.

Discussion

In this report we have presented the following points: first, we showed results indicating that S1, M1, PMd, and PMv all have MNs that have activity related to visually cued grip force; second, we have shown that the firing rate in each of these regions is also modulated by reward expectation during the post-cue period for cued reward level trials, and during the post-feedback time period for both cued and uncued reward level trials; third, that the MNs activity of visually cued grip force can coexist within single units that also code for reward level; fourth, that the MN activity during

observational trials, as compared to manual trials, could shift their temporal relationship predicting/responding to visually cued force about equally in either the predictive or responsive time lag directions; fifth, that the neural grip force tuning functions can be modulated by reward expectation in all 4 brain regions under study (S1, M1, PMd and PMv, see Fig.10) during both manual and observational trials.

To the best of our knowledge, we are reporting the first evidence of mirror neural responses to expected, or visually cued effort (grip force), within these sensorimotor regions. As the NHPs had a great deal of experience with the grip force task we expect the mirror responses were due to the visual cueing of force output that the NHPs had come to understand based on their manual trials. In Fig.7 we showed that the shift in peak correlation between cued force and neural time lag could be in either the direction expected for motor production, or that expected from sensory stimulation, which would be more in line with the initial MN work (Gallese et al. 1996), and the former more in line with movement rehearsal (Cisek and Kalaska 2004). We predict that such force MN activity could be seen in more natural settings if the context was understood by the NHPs, such as lifting heavy vs. light objects that they were familiar with, or perhaps when the NHP squeezes a deformable object, or observes such a grasp, again with knowledge of the object's physical properties. However, further work is needed to show such activity exists under more natural conditions within each of these regions. It should be noted that this type of prior knowledge being necessary for MN activity patterns is not new. Mirror neurons that encode subjective value in addition to grasping information clearly need the NHP to have familiarity with the object in some way to have formed a subjective value (Caggiano et al. 2012).

We have shown that reward modulation can occur post-cue, when the cue indicates the reward value of the current trial, as well as post-feedback when the reward level that was cued is delivered. When there is no reward cue given in uncued blocks there is no "post-cue" reward modulation as expected, but there is still post-feedback modulation in each of the 4 brain regions, and again

during both manual and observational trial types. Based on the evidence we have presented, we see that S1, M1, PMd and PMv contain units that encode reward expectation and reward itself, as has been shown previously for the task used in this work as well as other tasks for M1 (Zhao et al. 2018; Brandi T. Marsh et al. 2015; An et al. 2019; Ramakrishnan et al. 2017), indicating this reward modulation may be a generalized broadcast signal to regions involved in the ongoing sensorimotor planning and production of movement, as well as during observation of such movements, in a manner that can be predictive, as expected during mental simulation, and responsive to the visual stimuli, as expected for MNs as first described (Gallese et al. 1996). These results demonstrate that reward is encoded in the primary somatosensory cortex (S1) similarly to that shown for M1 in previous work (Brandi T. Marsh et al. 2015; Ramakrishnan et al. 2017) and premotor regions (M. R. Roesch and Olson 2007; Ramkumar et al. 2016). In addition, we have now shown such reward modulation simultaneously for M1, S1, PMd and PMv during both manual and observational trial types for the same single units tracked between tasks.

There are several limitations to the work presented here that should be addressed in future work. EMGs were not available for these particular datasets that allowed us to track single units between manual and observational trials, and therefore we can't state with certainty that the NHPs were not activating their arm muscles covertly, however, they were not making obvious movements, and did not have access to the force transducing handle, in addition, our previous studies found no correlation between EMGs and curser motion in observational trials of a reaching task (Brandi T. Marsh et al. 2015). In addition, we show in Fig.S.6 for both NHPs there was no significant EMG activity during observational trials on different days when the EMG signals were usable. The grip force output in the current task was generally phasic in nature with a bell-shaped profile, even if the cued amplitudes were different, the force profiles were still fairly stereotyped, and so it is possible that some other phasic neural response was allowing the regression models to predict force output, which was bell-shaped, by some non-force related phasic response, such as that

related to the cued reward information. However, the regression models did not fall apart in the uncued reward level task, which indicates at least cued reward does not explain our force decoding results. In addition, when we conducted analysis on the time series of just the peak force amplitude of each trial, we still obtained positive results showing MNs for force, although clearly not as strong as when using the fuller dataset including the force trajectories (see Fig.S8).

The work presented here has a practical application past basic neuroscience. We believe it is important to continue gaining a better understanding of encoded information, such as reward, within the sensorimotor cortices toward the development of a close-loop brain machine interface (BMI) for the restoration of motor control and beyond, such as towards a better understanding and tracking of psychological state of the individual. BMI neural signals are often recorded and decoded from a subset of S1, M1, PMd, and PMv while sensory feedback is obtained either by natural vision, or stimuli routed to S1, such as via the thalamus (Choi et al. 2016) for somatosensory feedback. It has recently been shown that reward expectation can change directional and force based tuning curves in M1 and S1 (Zhao et al. 2018; Ramakrishnan et al. 2017), and here we have shown that all of these brain regions are influenced by reward expectation, effort, or sensory feedback on expected effort, and therefore research into these relationship is warranted. Differentiating between mirror activity in these regions and intentional activity for movement is key towards making BMIs more stable with respect to the users intended movements compared to observed movements, and our future work will address these issues.

References

Alaerts, Kaat, Toon T. de Beukelaar, Stephan P. Swinnen, and Nicole Wenderoth. 2012. 'Observing How Others Lift Light or Heavy Objects: Time-Dependent Encoding of Grip Force in the Primary Motor Cortex'. *Psychological Research* 76 (4): 503–13. https://doi.org/10.1007/s00426-011-0380-1.

An, Junmo, Taruna Yadav, Mohammad Badri Ahmadi, Venkata S Aditya Tarigoppula, and Joseph Thachil Francis. 2018. 'Near Perfect Neural Critic from Motor Cortical Activity Toward an Autonomously Updating Brain Machine Interface'. In *2018 40th Annual International Conference of the IEEE Engineering in Medicine and Biology Society (EMBC)*, 73–76. https://doi.org/10.1109/EMBC.2018.8512274.

An, Junmo, Taruna Yadav, John P. Hessburg, and Joseph T. Francis. 2019. 'Reward Expectation Modulates Local Field Potentials, Spiking Activity and Spike-Field Coherence in the Primary Motor Cortex'. *ENeuro* 6 (3). https://doi.org/10.1523/ENEURO.0178-19.2019.

Atique, MD Moin, and Joseph T. Francis. 2019. 'Reward and Force Modulation of Neurons in the Primate Primary Somatosensory Cortex (S1)'. 2019. https://www.abstractsonline.com/pp8/#!/7883/presentation/59642.

Benjamini, Yoav, and Yosef Hochberg. 1995. 'Controlling the False Discovery Rate: A Practical and Powerful Approach to Multiple Testing'. *Journal of the Royal Statistical Society: Series B (Methodological)* 57 (1): 289–300. https://doi.org/10.1111/j.2517-6161.1995.tb02031.x.

Caggiano, V., L. Fogassi, G. Rizzolatti, A. Casile, M. A. Giese, and P. Thier. 2012. 'Mirror Neurons Encode the Subjective Value of an Observed Action'. *Proc Natl Acad Sci U S A* 109 (29): 11848–53. https://doi.org/10.1073/pnas.1205553109.

Chhatbar, Pratik Y., Lee M. von Kraus, Mulugeta Semework, and Joseph T. Francis. 2010. 'A Bio-Friendly and Economical Technique for Chronic Implantation of Multiple Microelectrode Arrays'. *Journal of Neuroscience Methods* 188 (2): 187–94. https://doi.org/10.1016/j.jneumeth.2010.02.006.

Choi, John S., Austin J. Brockmeier, David B. McNiel, Lee M. von Kraus, José C. Príncipe, and Joseph T. Francis. 2016. 'Eliciting Naturalistic Cortical Responses with a Sensory Prosthesis via Optimized Microstimulation'. *Journal of Neural Engineering* 13 (5): 056007. https://doi.org/10.1088/1741-2560/13/5/056007.

Cisek, P., and J. F. Kalaska. 2004. 'Neural Correlates of Mental Rehearsal in Dorsal Premotor Cortex'. *Nature* 431 (7011): 993–96. https://doi.org/10.1038/nature03005.

Cohen, Jeremiah Y., Sebastian Haesler, Linh Vong, Bradford B. Lowell, and Naoshige Uchida. 2012. 'Neuron-Type-Specific Signals for Reward and Punishment in the Ventral Tegmental Area'. *Nature* 482 (7383): 85–88. https://doi.org/10.1038/nature10754.

Dushanova, Juliana, and John Donoghue. 2010. 'Neurons in Primary Motor Cortex Engaged during Action Observation'. *European Journal of Neuroscience* 31 (2): 386–98. https://doi.org/10.1111/j.1460-9568.2009.07067.x.

Gallese, V., L. Fadiga, L. Fogassi, and G. Rizzolatti. 1996. 'Action Recognition in the Premotor Cortex'. *Brain: A Journal of Neurology* 119 (Pt 2) (April): 593–609. https://doi.org/10.1093/brain/119.2.593.

Glimcher, Paul W., Ernst Fehr, Colin Camerer, and Russell Alan Poldrack, eds. 2008. *Neuroeconomics: Decision Making and the Brain*. 1 edition. Amsterdam Boston Heidelberg London New York Oxford Paris San Diego San Francisco Singapore Sydney Tokyo: Academic Press.

Kipke, D.R., R.J. Vetter, J.C. Williams, and J.F. Hetke. 2003. 'Silicon-Substrate Intracortical Microelectrode Arrays for Long-Term Recording of Neuronal Spike Activity in Cerebral

Cortex'. *IEEE Transactions on Neural Systems and Rehabilitation Engineering* 11 (2): 151–55. https://doi.org/10.1109/TNSRE.2003.814443.

Kretzberg, Jutta, Thomas Coors, and Julia Furche. 2009. 'Comparison of Valley Seeking and T-Distributed EM Algorithm for Spike Sorting'. *BMC Neuroscience* 10 (1): P47. https://doi.org/10.1186/1471-2202-10-S1-P47.

Maranesi, M., A. Livi, L. Fogassi, G. Rizzolatti, and L. Bonini. 2014. 'Mirror Neuron Activation Prior to Action Observation in a Predictable Context'. *J Neurosci* 34 (45): 14827–32. https://doi.org/10.1523/JNEUROSCI.2705-14.2014.

Marsh, B. T., V. S. Tarigoppula, C. Chen, and J. T. Francis. 2015. 'Toward an Autonomous Brain Machine Interface: Integrating Sensorimotor Reward Modulation and Reinforcement Learning'. *J Neurosci* 35 (19): 7374–87. https://doi.org/10.1523/JNEUROSCI.1802-14.2015.

Marsh, Brandi T., Venkata S. Aditya Tarigoppula, Chen Chen, and Joseph T. Francis. 2015. 'Toward an Autonomous Brain Machine Interface: Integrating Sensorimotor Reward Modulation and Reinforcement Learning'. *Journal of Neuroscience* 35 (19): 7374–87. https://doi.org/10.1523/JNEUROSCI.1802-14.2015.

Mazurek, Kevin A., Adam G. Rouse, and Marc H. Schieber. 2018. 'Mirror Neuron Populations Represent Sequences of Behavioral Epochs During Both Execution and Observation'. *Journal of Neuroscience* 38 (18): 4441–55. https://doi.org/10.1523/JNEUROSCI.3481-17.2018.

McNiel, David B., John S. Choi, John P. Hessburg, and Joseph T. Francis. 2016. 'Reward Value Is Encoded in Primary Somatosensory Cortex and Can Be Decoded from Neural Activity during Performance of a Psychophysical Task'. In , 3064–67. IEEE.

McNiel, David, Mohammad Bataineh, John Choi, John Hessburg, and Joseph Francis. 2016. 'Classifier Performance in Primary Somatosensory Cortex Towards Implementation of a Reinforcement Learning Based Brain Machine Interface'. In *2016 32nd Southern Biomedical Engineering Conference (SBEC)*, 17–18. https://doi.org/10.1109/SBEC.2016.19.

Murray, G. K., P. R. Corlett, L. Clark, M. Pessiglione, A. D. Blackwell, G. Honey, P. B. Jones, E. T. Bullmore, T. W. Robbins, and P. C. Fletcher. 2008. 'Substantia Nigra/Ventral Tegmental Reward Prediction Error Disruption in Psychosis'. *Molecular Psychiatry* 13 (3): 267–76. https://doi.org/10.1038/sj.mp.4002058.

Pleger, Burkhard, Felix Blankenburg, Christian C. Ruff, Jon Driver, and Raymond J. Dolan. 2008. 'Reward Facilitates Tactile Judgments and Modulates Hemodynamic Responses in Human Primary Somatosensory Cortex'. *Journal of Neuroscience* 28 (33): 8161–68. https://doi.org/10.1523/JNEUROSCI.1093-08.2008.

Pohlmeyer, Eric A., Babak Mahmoudi, Shijia Geng, Noeline Prins, and Justin C. Sanchez. 2012. 'Brain-Machine Interface Control of a Robot Arm Using Actor-Critic Rainforcement Learning'. In *2012 Annual International Conference of the IEEE Engineering in Medicine and Biology Society*, 4108–11. https://doi.org/10.1109/EMBC.2012.6346870.

Pohlmeyer, Eric A., Babak Mahmoudi, Shijia Geng, Noeline W. Prins, and Justin C. Sanchez. 2014. 'Using Reinforcement Learning to Provide Stable Brain-Machine Interface Control Despite Neural Input Reorganization'. *PLoS ONE* 9 (1). https://doi.org/10.1371/journal.pone.0087253.

Quigley, Morgan, Ken Conley, Brian Gerkey, Josh Faust, Tully Foote, Jeremy Leibs, Rob Wheeler, and Andrew Y. Ng. 2009. 'ROS: An Open-Source Robot Operating System'. In *ICRA Workshop on Open Source Software*, 3:5. Kobe, Japan.

Ramakrishnan, Arjun, Yoon Woo Byun, Kyle Rand, Christian E. Pedersen, Mikhail A. Lebedev, and Miguel A. L. Nicolelis. 2017. 'Cortical Neurons Multiplex Reward-Related Signals along with Sensory and Motor Information'. *Proceedings of the National Academy of Sciences* 114 (24): E4841–50. https://doi.org/10.1073/pnas.1703668114.

Ramkumar, Pavan, Brian Dekleva, Sam Cooler, Lee Miller, and Konrad Kording. 2016. 'Premotor and Motor Cortices Encode Reward'. Edited by William W Lytton. *PLOS ONE* 11 (8): e0160851. https://doi.org/10.1371/journal.pone.0160851.

Roesch, M. R., and C. R. Olson. 2007. 'Neuronal Activity Related to Anticipated Reward in Frontal Cortex: Does It Represent Value or Reflect Motivation?' *Ann N Y Acad Sci* 1121 (December): 431–46. https://doi.org/10.1196/annals.1401.004.

Roesch, Matthew R., and Carl R. Olson. 2003. 'Impact of Expected Reward on Neuronal Activity in Prefrontal Cortex, Frontal and Supplementary Eye Fields and Premotor Cortex'. *Journal of Neurophysiology* 90 (3): 1766–89. https://doi.org/10.1152/jn.00019.2003.

Rolls, Edmund T. 2014. *Emotion and Decision-Making Explained*. First edition. Oxford ; New York, NY: Oxford University Press.

Sanchez, Justin C., Aditya Tarigoppula, John S. Choi, Brandi T. Marsh, Pratik Y. Chhatbar, Babak Mahmoudi, and Joseph T. Francis. 2011. 'Control of a Center-out Reaching Task Using a Reinforcement Learning Brain-Machine Interface'. In *2011 5th International IEEE/EMBS Conference on Neural Engineering*, 525–28. https://doi.org/10.1109/NER.2011.5910601.

Sato, Makoto, and Okihide Hikosaka. 2002. 'Role of Primate Substantia Nigra Pars Reticulata in Reward-Oriented Saccadic Eye Movement'. *Journal of Neuroscience* 22 (6): 2363–73. https://doi.org/10.1523/JNEUROSCI.22-06-02363.2002.

Schultz, Wolfram, Peter Dayan, and P. Read Montague. 1997. 'A Neural Substrate of Prediction and Reward'. *Science* 275 (5306): 1593–99. https://doi.org/10.1126/science.275.5306.1593.

Tkach, Dennis, Jacob Reimer, and Nicholas G. Hatsopoulos. 2007. *Journal of Neuroscience* 27 (48): 13241–50. https://doi.org/10.1523/JNEUROSCI.2895-07.2007.

Tremblay, Léon, and Wolfram Schultz. 1999. 'Relative Reward Preference in Primate Orbitofrontal Cortex'. *Nature* 398 (6729): 704–8. https://doi.org/10.1038/19525.

Vigneswaran, G., R. Philipp, R. N. Lemon, and A. Kraskov. 2013. 'M1 Corticospinal Mirror Neurons and Their Role in Movement Suppression during Action Observation'. *Curr Biol* 23 (3): 236–43. https://doi.org/10.1016/j.cub.2012.12.006.

Vigneswaran, Ganesh, Roland Philipp, Roger N. Lemon, and Alexander Kraskov. 2013. 'M1 Corticospinal Mirror Neurons and Their Role in Movement Suppression during Action Observation'. *Current Biology* 23 (3): 236–43. https://doi.org/10.1016/j.cub.2012.12.006.

Yuan, Yuan, Chenhui Yang, and Jennie Si. 2012. 'The M-Sorter: An Automatic and Robust Spike Detection and Classification System'. *Journal of Neuroscience Methods* 210 (2): 281–90. https://doi.org/10.1016/j.jneumeth.2012.07.012.

Zaghloul, Kareem A., Justin A. Blanco, Christoph T. Weidemann, Kathryn McGill, Jurg L. Jaggi, Gordon H. Baltuch, and Michael J. Kahana. 2009. 'Human Substantia Nigra Neurons Encode Unexpected Financial Rewards'. *Science* 323 (5920): 1496–99. https://doi.org/10.1126/science.1167342.

Zhao, Yao, John P. Hessburg, Jaganth Nivas Asok Kumar, and Joseph T. Francis. 2018. 'Paradigm Shift in Sensorimotor Control Research and Brain Machine Interface Control: The Influence of Context on Sensorimotor Representations'. *Frontiers in Neuroscience* 12. https://doi.org/10.3389/fnins.2018.00579.

SUPPLEMENTARY INFORMATION

Mirror Neurons are Modulated by Reward expectation and Grip Force in the Sensorimotor Cortices (S1, M1, PMd, PMv)

Abbreviated title:

Md Moin Uddin Atique[2] and Joseph Thachil Francis[1-3]

Correspondence: Joey199us@gmail.com

Acknowledgements: Research was supported by NIH 1R01NS092894-01, NSF IIS-17 1527558, DARPA REPAIR Project N66001-10-C-2008.

[1]Department of Biomedical Engineering, Cullen College of Engineering, The University of Houston, Houston, TX 77204, United States;

[2] Department of Electrical and Computer Engineering, Cullen College of Engineering, The University of Houston, Houston, TX 77204, United States;

[3] Lead Contact- jtfracis@uh.edu

Supplementary Information

Algorithm for Linear Regression: The following algorithm shows the two-step process of collecting a subset of units significant for force to achieve a comparatively better prediction of force using linear regression. **Fig.S1**

Step 1: Sort Units in ascending order of p-value

1. Total number of units ***N***
2. Used 80% fitting set and checked the significance (F-test) of fitting for all ***N*** (one unit at a time) units.
   Model: $\mathbf{y_f} = \boldsymbol{\alpha X}_{fr}^{1} + \boldsymbol{b}$ eq. 1
3. Collect all significant units $\boldsymbol{n}=[\boldsymbol{n_1}, \boldsymbol{n_2}, \boldsymbol{n_3} \ldots\ldots]$ with (p-value< 0.05).
4. Sort ***n*** units in ascending order by p-value.

Step 2: Add units that increase prediction

1. Determine R.^2 value for each unit from step #1. First fit with 80% fitting set then determine R.^2 on 10% validation set.
   Model: $\mathbf{y_f} = \boldsymbol{\alpha}\mathbf{X_{fr}} + \boldsymbol{\beta}$ eq. 2
2. If R.^2 fit increases add unit, if not, don't.
3. Repeat step 2 for all ***n***

Final Prediction:

1. Fit 90% fitting set using neural data from the above units that added to the R.^2 of the fitting dataset.
2. Determine the R^2 using the 10% test set.

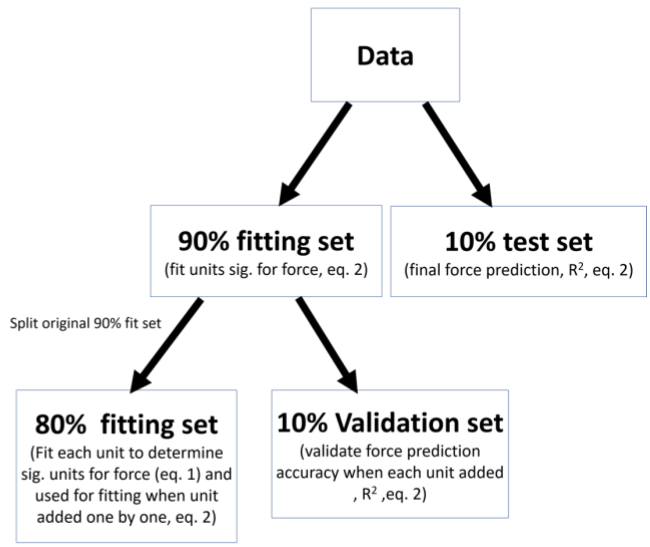

Observation Results on force:

This figure shows raster plots of some example units from each of the 4 cortices during grip force onset taken from observation blocks showing the full average force time period.

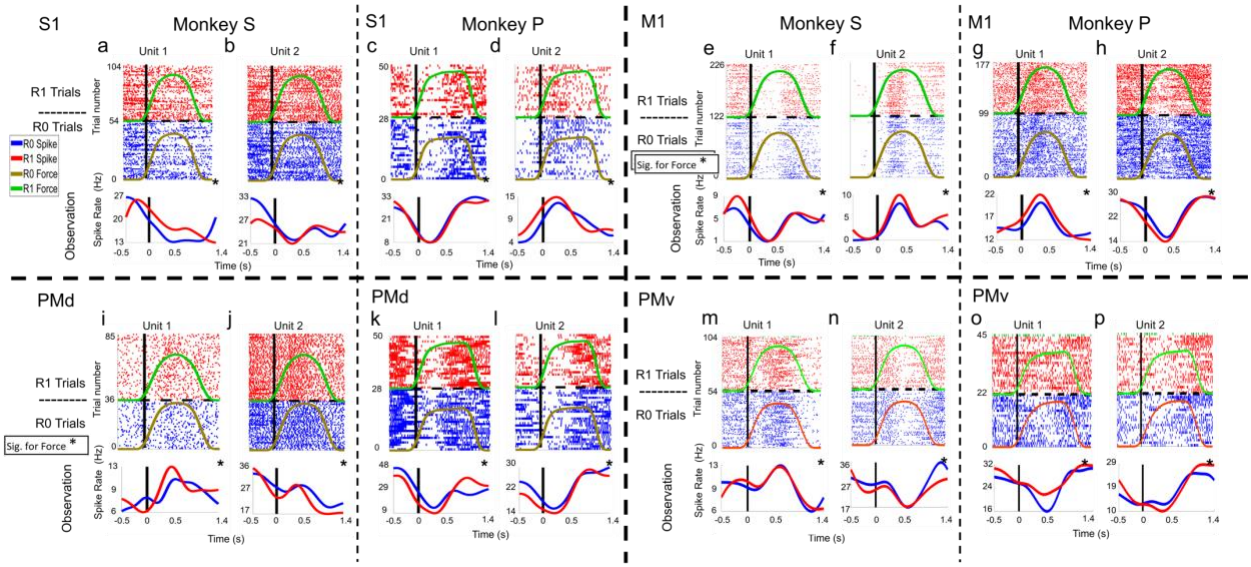

Figure S2: Raster plots for units from S1 (plots a, b, c and d), M1 region (plots e, f, g and h), PMd (plots i, j, k and l) and PMv (plots m, n, o and p) are shown for NHPs S and P. These plots show the grip force values indicated to NHPs during observational blocks. The black bold line on each raster and spike rate plot shows the onset of force and the dotted horizontal line divides R1 (top, red) and R0 (bottom, blue) trials.

Time Dependent Correlation Analysis:

The time dependent peak correlation plots for all the blocks are given here on the following figure. Only the units tracked through all manual and observational blocks and were significant for force are shown here. For each NHP the trend of the distribution of units is similar between blocks but different for each NHP specially for the manual blocks. See Fig.7 for differences between block types.

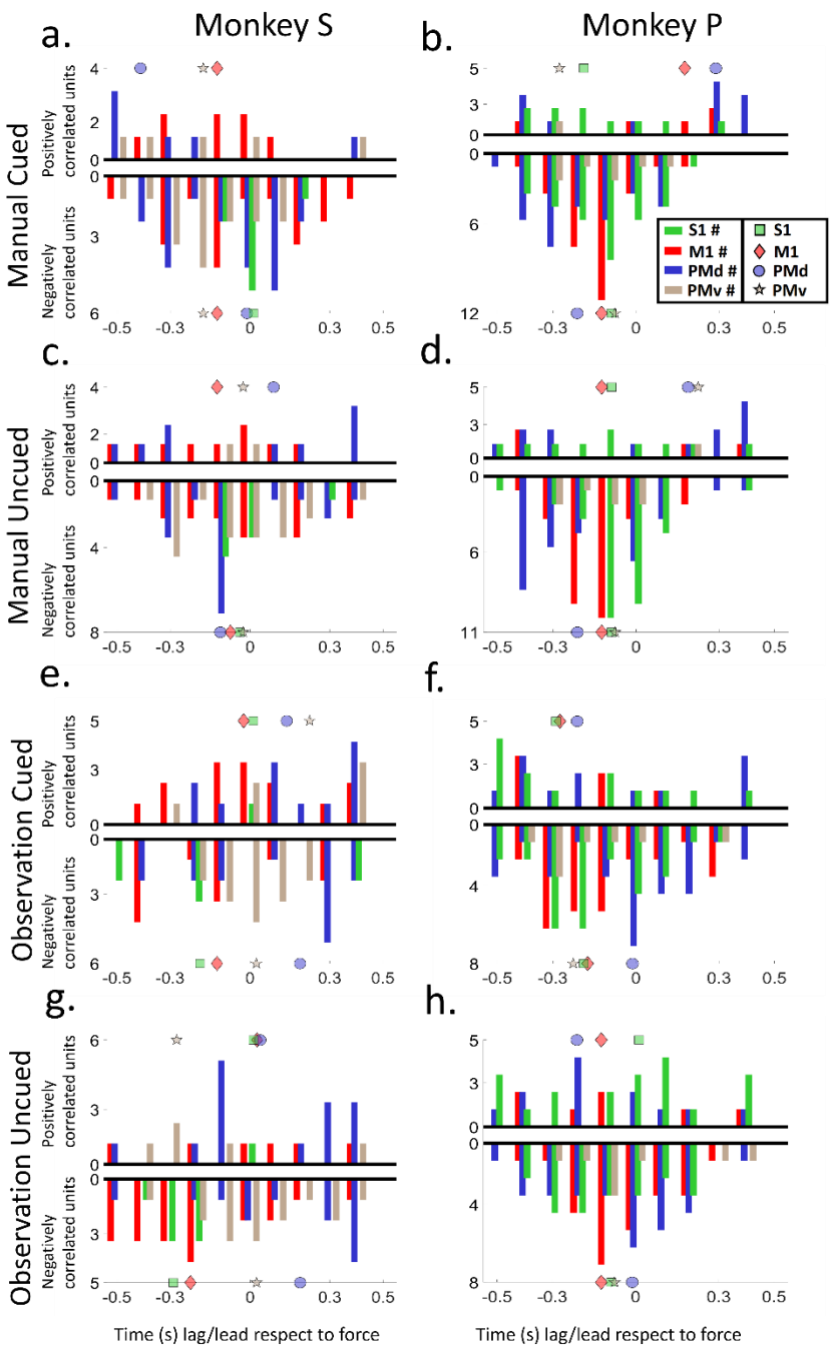

Figure S3: The number of units that had their highest correlation between force and spike rate for each time bin are shown leading (0.5s before) or lagging (0.5s after) each force value (100ms non-overlapping time bins). Units significant (F-test, $p < 0.05$) on all block types were plotted in the time bin where their correlation coefficient with force was most negative or positive. The y-axis is

representing the number of units (positively correlated units on the upper side and negatively correlated units on the lower). The x-axis is representing the time lag/lead for which the maximum correlation was found. Units from S1 (a, b), M1 (c, d), PMd (e, f) and PMv (g, h) cortex are given on each plot and the legend is showing the color diagram for each cortex.

Distribution of Significant Correlation Time Lags Between Neural Activity and Force:

The following figure is showing the time shift of significant peak correlation from manual cued blocks to manual uncued blocks and from observation cued blocks to observation uncued blocks. See Fig.7 for more of such plots.

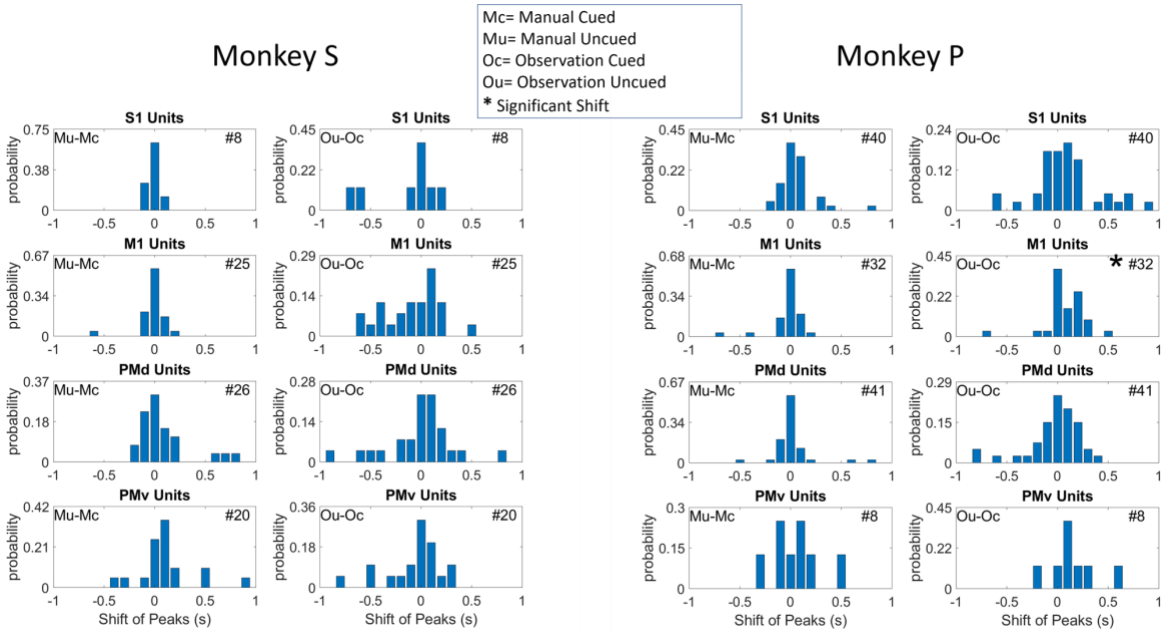

Figure S4: The shift of peak force correlation from manual to manual and observational to observational block. Bar plots showing the shift of peak correlation between Manual blocks and Observational blocks for S1, M1, PMd and PMv cortex for individual MNs. The shift from a block type to another block type is given on the left to of each figure and short form of the block type (Mc= Manual Cued, Mu= Manual Uncued, Oc= Observation Cued, Ou= Observation Uncued) was used. The number of units used is included on the upper left corner of each subplot. An Asterix (*) symbol before the number of units represents a significant shift in histogram between the blocks

used for that subplot. Shift was calculated by subtracting the manual histogram for cued from the Manual histogram for uncued and similarly for the observational cases.

Regression on additional observational blocks:

Table shows the regression data analysis for NHP S and P. The table contains the R-square value for model fit given in equation 1 and the corresponding p-value and F-statistic. The R-squared value for prediction and its p-value is also shown on the table. This table contains two additional observational blocks that were recorded on a different day.

Table S1: Regression Model Output for NHP S & P for the two additional observational blocks recorded on a different day with units we could not track from the previous data sets.

NHP S - S1					
Block	R-fit	p-value	F-stat	R-predict	p-value
Observation Cued	0.28	3e-91	3.81	0.19	8.3e-21
Observation Uncued	0.34	4.3e-154	4.79	0.04	9.3e-6

NHP P – S1					
Block	R-fit	p-value	F-stat	R-predict	p-value
Observation Cued	0.46	1.3e-229	8.34	0.27	1.9e-26
Observation Uncued	0.53	0	10.09	0.13	1.8e-14

NHP S – M1					
Block	R-fit	p-value	F-stat	R-predict	p-value
Observation Cued	0.65	0	11.59	0.6	2.6e-87
Observation Uncued	0.76	0	21.19	0.66	4.3e-113

NHP P – M1					
Block	R-fit	p-value	F-stat	R-predict	p-value
Observation Cued	0.61	0	13.19	0.55	2.7e-64
Observation Uncued	0.69	0	18.07	0.55	3.1e-75

NHP S – PMd					
Block	R-fit	p-value	F-stat	R-predict	p-value
Observation Cued	0.53	1.9e-273	6.63	0.36	2.7e-43
Observation Uncued	0.67	0	11.57	0.39	0.55

NHP P – PMd					
Block	R-fit	p-value	F-stat	R-predict	p-value
Observation Cued	0.5	6.4e-274	10	0.52	6.3e-59
Observation Uncued	0.55	0	13.14	0.37	2e-44

NHP S – PMv	NHP P – PMv

Block	R-fit	p-value	F-stat	R-predict	p-value
Observation Cued	0.6	0	11.84	0.72	5.7e-121
Observation Uncued	0.8	0	34.11	0.72	6.1e-134

Block	R-fit	p-value	F-stat	R-predict	p-value
Observation Cued	0.35	3.5e-197	11.24	0.28	4.9e-27
Observation Uncued	0.46	0	13.18	0.36	1.4e-42

Table S2: Regression model statistics for Fig. 5 in the main text.

Table S2: Regression Model Output for NHPs S & P

NHP S - S1

Block	R^2-fit	p-value	F-stat	R^2-predict	p-value
Manual Cued	0.91	0	$F_{550,2173}$ 39.83	0.78	1.9e-101
Manual Uncued	0.89	0	$F_{540,3597}$ 51.68	0.82	3.5e-173
Obs Cued	0.34	7.4e-40	$F_{250,1330}$ 3.32	**0.11**	9.5e-6
Obs Uncued	0.29	9.4e-46	$F_{300,1679}$ 3.47	**0.14**	7.8e-9

NHP P – S1

Block	R^2-fit	p-value	F-stat	R^2-predict	p-value
Manual Cued	0.78	0	$F_{320,2142}$ 24.19	0.84	2.26e-109
Manual Uncued	0.9	0	$F_{470,2528}$ 46.77	0.87	4.6e-148
Obs Cued	0.68	5e-88	$F_{220,707}$ 7.12	**0.66**	1.4e-25
Obs Uncued	0.47	2.3e-42	$F_{220,652}$ 4.6	**0.15**	9.5e-5

NHP S – M1

Block	R^2-fit	p-value	F-stat	R^2-predict	p-value
Manual Cued	0.92	0	$F_{590,2133}$ 44.24	0.80	7.8e-109
Manual Uncued	0.93	0	$F_{530,3607}$ 85.7	0.83	1.2e-180
Obs Cued	0.69	1.7e-147	$F_{240,1340}$ 6.91	**0.51**	1.6e-28
Obs Uncued	0.65	1.2e-197	$F_{350,1629}$ 8.19	**0.45**	1.8e-30

NHP P – M1

Block	R^2-fit	p-value	F-stat	R^2-predict	p-value
Manual -Cued	0.80	0	$F_{360,2102}$ =23.71	0.87	5.58e-123
Manual -Uncued	0.89	0	$F_{440,2558}$ 46.22	0.87	1.6e-151
Obs Cued	0.76	6.3e-96	$F_{300,627}$ 7.29	**0.56**	7e-20
Obs Uncued	0.57	4.5e-52	$F_{180,692}$ 4.81	**0.32**	1.5e-09

NHP S –PMd

NHP P – PMd

Block	R^2-fit	p-value	F-stat	R^2-predict	p-value
Manual Cued	0.92	0	$F_{550,2173}$ 44.25	0.84	1.3e-122
Manual Uncued	0.92	0	$F_{640,3497}$ 58.86	0.83	9.1e-181
Obs Cued	0.66	6.3e-172	$F_{270,1310}$ 8.99	**0.54**	1.5e-31
Obs Uncued	0.73	2.5e-282	$F_{330,1649}$ 11.95	**0.61**	6.4e-47

Block	R^2-fit	p-value	F-stat	R^2-predict	p-value
Manual Cued	0.85	0	$F_{260,2202}$ 47.17	0.94	4.9e-164
Manual Uncued	0.93	0	$F_{540,2458}$ 63.09	0.91	6.4e-175
Obs Cued	0.73	1.3e-117	$F_{240,627}$ 9.79	**0.66**	1.4e-25
Obs Uncued	0.72	4.7e-82	$F_{200,672}$ 6.71	**0.36**	7.3e-11

NHP S –PMv

Block	R^2-fit	p-value	F-stat	R^2-predict	p-value
Manual Cued	0.83	0	$F_{430,2293}$ 26.72	0.77	2.3
Manual Uncued	0.87	0	$F_{610,3527}$ 40.29	0.67	4.4e-112
Obs Cued	0.81	4e-265	$F_{320,1260}$ 13.65	**0.69**	4.9e-46
Obs Uncued	0.86	0	$F_{430,1549}$ 16.25	**0.77**	7.1e-71

NHP P – PMv

Block	R^2-fit	p-value	F-stat	R^2-predict	p-value
Manual Cued	0.61	5.3e-308	$F_{24,2222}$ 14.26	0.53	9.3e-47
Manual Uncued	0.6	0	$F_{160,2838}$ 26.31	0.57	5.6e-63
Obs Cued	0.43	1.2e-60	$F_{80,847}$ 7.89	**0.29**	2.7e-09
Obs Uncued	0.33	7.9e-45	$F_{80,792}$ 8.15	**0.40**	2.9e-12

Table S2: Displays results from the regression analysis for NHPs S and P between neural activity and force trajectories. The table contains the R-square value for the model (eq. 2) fit and prediction including their corresponding p-values and F-statistics. We have used bold text for the prediction during observation tasks. Note all single units were followed through each of the 4 task types on a given day. From table 1 it appears that these brain regions are representing force during both the manual trails and the observational versions of these trials. In Fig.6 we show the number of single units that significantly predict force during both manual and observational trails indicating that these same units are representing this information to some extent during both manual and observed movements, which may represent a new form of mirror neuron activity.

Table S3: Units with significantly different slopes for the force tuning curves between R0 and R1. The values in parenthesis show the adjusted significant units after Benjamini and Hochberg's method accounting for the false discovery rate was applied. The BH method applied for number of hypothesis is described in the method section titled "grip force tuning curve analysis".

	S1 #	S1 %	M1 #	M1 %	PMd #	PMd %	PMv #	PMv %
NHP S Manual	25 (24)	19% (18%)	32 (31)	23% (22%)	38 (38)	28% (28%)	29 (25)	18% (15%)
NHP P Manual	31 (25)	24% (19%)	23 (23)	20% (20%)	33 (32)	28% (10%)	13 (13)	15% (15%)
NHP S Obs.	5 (4)	5% (4%)	3 (3)	3% (3%)	2 (2)	2% (2%)	2 (2)	2% (2%)
NHP P Obs.	2 (1)	2% (1%)	2 (2)	2% (2%)	4 (4)	4% (4%)	2 (2)	3% (3%)

Table S4: Units with significantly different y-intercept for the force tuning curves for R0 and R1. The values in parenthesis show the adjusted significant units after Benjamini and Hochberg's method accounting for the false discovery rate was applied. The BH method applied for number of Hypothesis is described in the method section titled "grip force tuning curve analysis".

	S1 #	S1 %	M1 #	M1 %	PMd #	PMd %	PMv #	PMv %
NHP S Manual	29 (27)	21% (20%)	45 (40)	32% (28%)	50 (49)	36% (36%)	36 (33)	22% (20%)
NHP P Manual	18 (16)	14% (12%)	24 (24)	21% (17%)	33 (31)	28% (26%)	9 (9)	11% (15%)
NHP S Obs.	4 (4)	4% (4%)	5 (5)	4% (4%)	3 (3)	3% (3%)	6 (5)	5% (4%)
NHP P Obs.	1 (0)	1% (0%)	2 (2)	2% (2%)	4 (3)	4% (3%)	2 (2)	3% (3%)

Spike Rate vs Force (Manual)

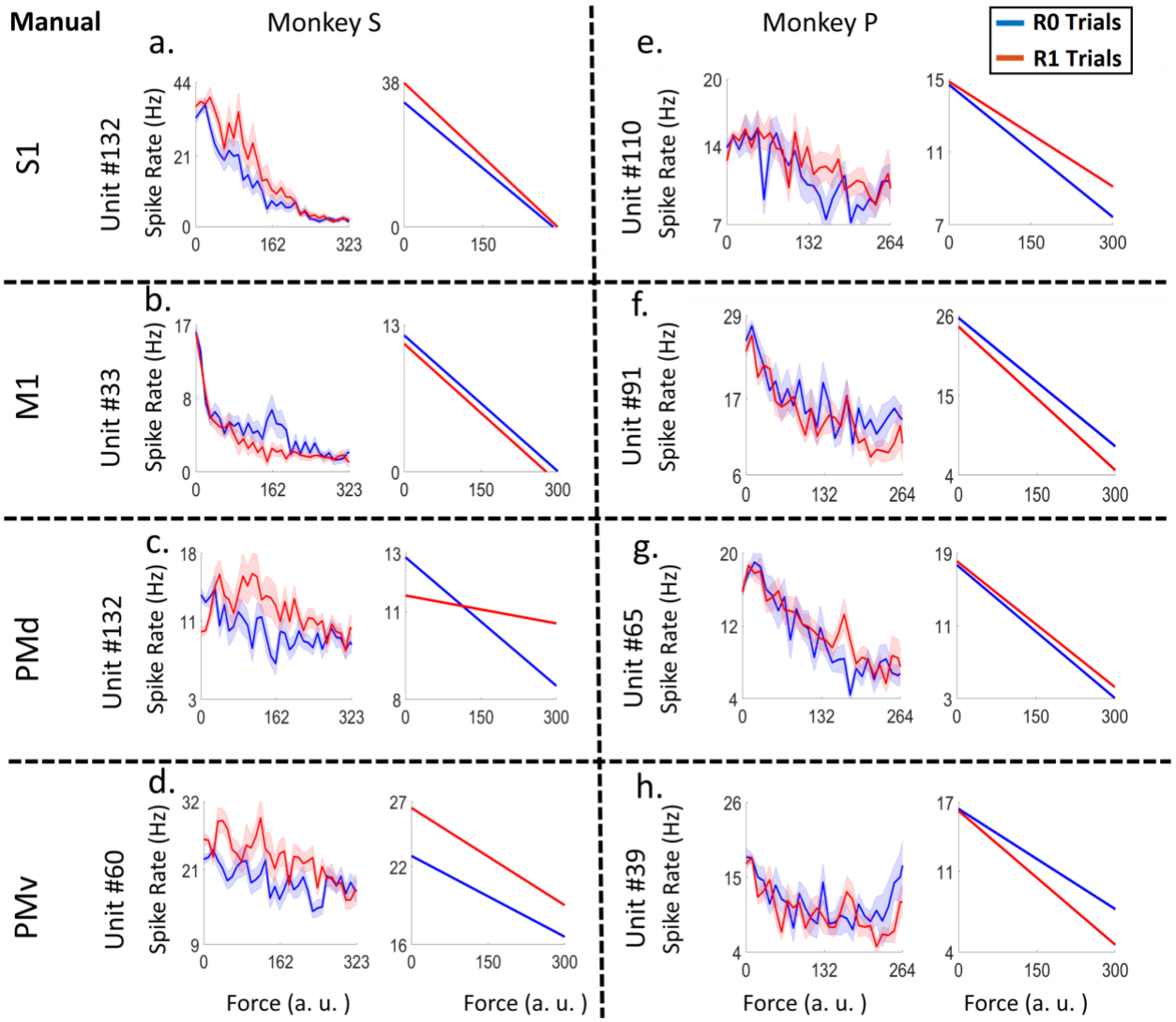

Figure. S5: Plots of spike rate vs force (left subplots) and their linear tuning curve (right subplots) for Grip force manual trials as compared to Fig.9 for observational. The subplots show example units from S1 (plot *a, e*), M1 (plot *b, f*), PMd (plot *c, g*) and PMv (plot *d, h*) cortices of both NHPs (for NHP S plots *a, b, c* and *d* and for NHP P plots *e, f, g* and *h*). The units presented here showed a significant difference between R0 and R1 groups (ANCOVA, F-test, $p<0.05$) force tuning curves during observation of robotic manipulator applying grip force on a force sensor. Red lines indicate rewarding trials (R1) and blue indicate non-rewarding trials (R0).

EMG Analysis

The data used in the main text had corrupted EMG and we were unable to confirm whether the NHPs were still using their arm muscles during the observation task, however, from observation notes of the experiments, and the clear decrease in activity seen in Figs 3-4 of the main text, and the fact that the NHPs could not reach for, or touch the force transducing handle, we do not believe the NHPs were physically rehearsing grip movements during observation. In addition, as seen below in Fig.S8, EMG on other days from these same NHPs was available during observation trials and did show any obvious activation patterns in the mean activity, however, it appears there was some small and insignificant increase in biceps for NHP P. The neural results of these below data sets held to that shown in the main text and figs. This does not rule out the NHPs covertly imagining movement, which was addressed in the main text.

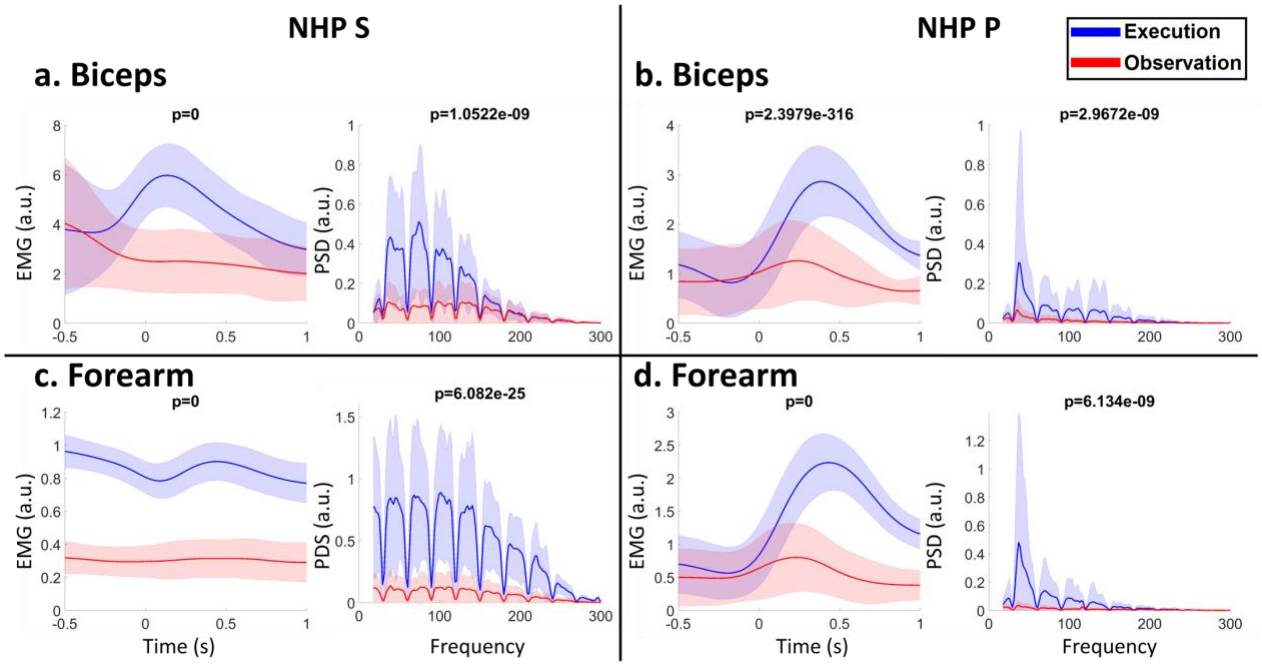

Figure S6: EMG collected from the Biceps (section a and b) and Forearm (section c and d) of NHP S (section a and c) and P (section b and d) recorded on different days. The blue color represents manual blocks (execution) and red is for observation. On each of four sections a, b, c and d, left

plots show the mean EMG (0.5s pre-force onset to 1s post force onset activity) for all the trials with standard deviation as shaded error bar. The right plots are showing the mean power spectral density (PSD) with standard deviation for same data. A band pass filter was applied on the EMG for the power line noise and its harmonics (30Hz, 60Hz, 90Hz… etc) and the effect of that can be seen in the PSD plots (b). The p-value for the significance test between the mean manual and observational is given on the title of each subplot.

Autocorrelation on the reward level target sequence:

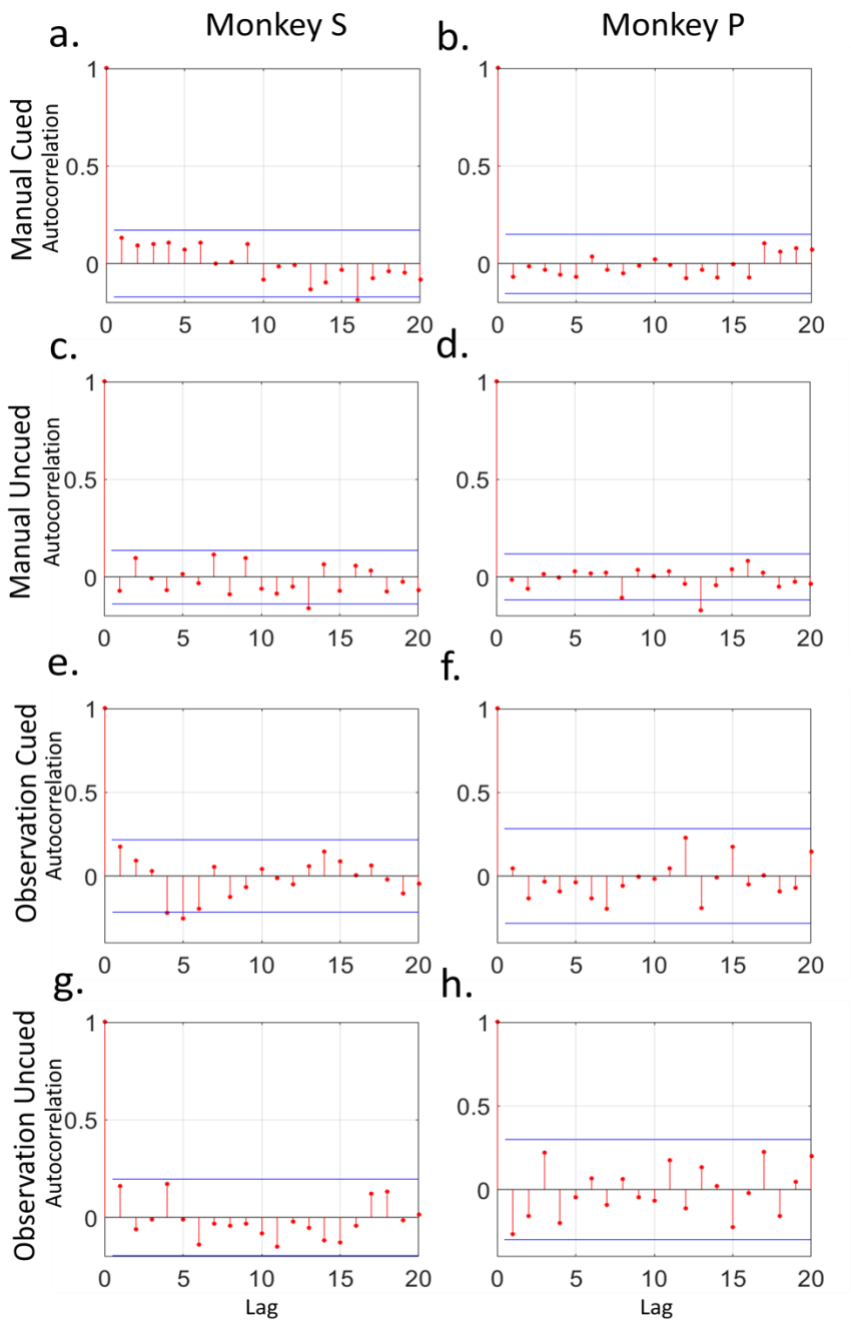

Figure S7: Autocorrelation on the reward level target sequence (R0 and R1) of trials for all the blocks. Plot a, c, e, and g are for NHP S and b, d, f, and h is for NHP P. The block type is given on the right side of each row. The x-axis represents lag and y axis represents corresponding autocorrelation.

Significant units for Peak Grip force:

As force profiles were stereotypical smooth Gaussian-like profiles, we wanted to make sure our regression model fits and predictions were meaningful, and not solely due to a unit having a phasic response that could be used to fit the stereotypical waveform. Therefore, we determined how neural activity correlated with the peak values of the Gaussian-shaped force profiles during each trial. We considered force values around the peak force applied on each trial (three values around the peak including the peak value) and we placed neural data, centered around each of them, into ten 100ms non-overlapping bins from 500ms pre peak force to 500ms post peak force neural activity. Each MN (figure 6 on the main manuscript) was tested for peak force significance (F-test, BH corrected for number of Hypothesis=4) by fitting a linear regression model with peak force values and spike rate for each of the ten bins. The red bars on figure S8 are showing significant units for peak grip force activity. The blue bars are showing the units significant for all the grip force values as described on the method section of the main manuscript titled "*Force trajectory Prediction*".

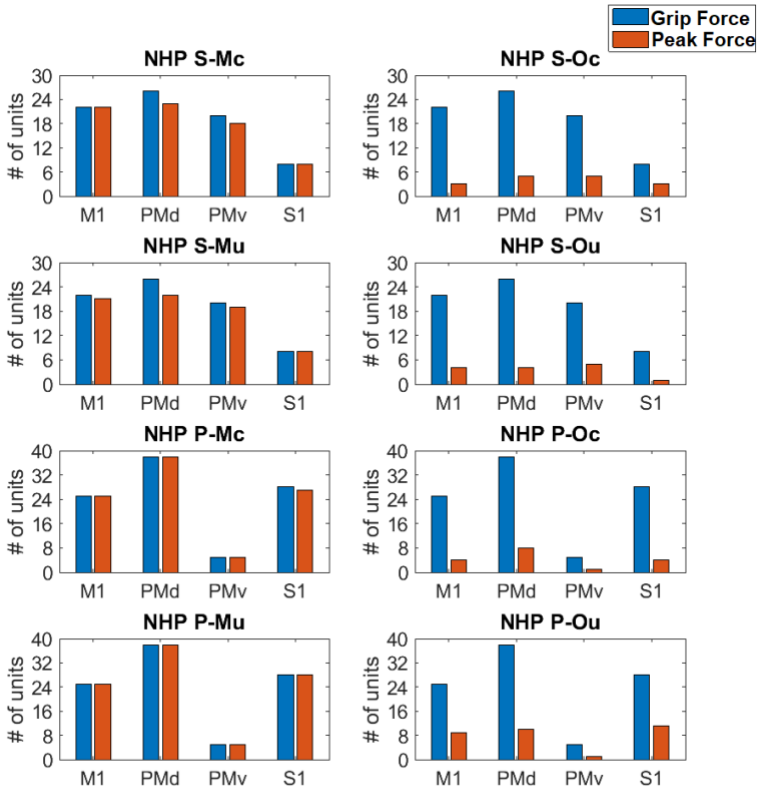

Figure S8: Significant mirror neurons (MN) for grip force (blue) and peak grip force (red) for Cued and uncued Manual (left subplots) and Observational (right subplots) block from NHP P (bottom four subplots) and S (top four subplots). The blue bars are representing units significant for grip force (F-test, BH corrected for number of Hypothesis) and red bars are representing units significant for peak grip force values (F-test, BH corrected for number of Hypothesis). The abbreviations on the subplot titles have the following meanings where Mc = Manual cued block, Oc = Observation cued block, Mu = Manual uncued block, and Ou = Observation uncued block. This plot is showing the mirror neuron units information from the Figure 6 of the main manuscript.